

Elsevier Editorial System(tm) for Renewable & Sustainable Energy Reviews
Manuscript Draft

Manuscript Number:

Title: Review of solid-liquid phase change materials and their encapsulation technologies

Article Type: Review Article

Keywords: Phase change material (PCM), micro-/nano-encapsulation technology, evaluation technologies

Corresponding Author: Mr. Weiguang Su,

Corresponding Author's Institution: University of Nottingham Ningbo China

First Author: Weiguang Su

Order of Authors: Weiguang Su; Jo Darkwa; Georgios KOKOGIANNAKIS

Abstract: Various types of solid-liquid phase change materials (PCMs) have been reviewed for thermal energy storage applications. The review has shown that organic solid-liquid PCMs have much more advantages and capabilities than inorganic PCMs but do possess low thermal conductivity and density as well as being flammable. Encapsulation technologies and shell materials have also been examined and limitations established. The morphology of particles were identified as a key influencing factor on the thermal and chemical stability and the mechanical strength of encapsulated PCMs. Enhancement methods and standardization of testing procedures for microencapsulated PCMs are therefore being encouraged.

Suggested Reviewers: Anton Ianakiev
Nottingham Trent University
anton.ianakiev@ntu.ac.uk

Robert Critoph
University of Warwick
R.E.Critoph@warwick.ac.uk

Guohui Gan
The University of Nottingham
guohui.gan@nottingham.ac.uk

Opposed Reviewers:

Centre for Sustainable Energy Technologies (CSET), University of Nottingham-Ningbo, Ningbo-China

The Editor
Renewable & Sustainable Energy Reviews

January 15, 2014

Dear Editor,

Please see attached a copy of a manuscript entitled "**Review of solid-liquid phase change materials and their encapsulation technologies**" for consideration and publication in the journal.

This paper is a review paper focusing on solid-liquid phase change materials and micro-/nano-encapsulated phase change material fabrication technologies. This is part of a research to develop a high quality microencapsulated phase change material for thermal energy storage in university of Nottingham Ningbo China.

The first author is Mr Weiguang Su, who is the correspondence author, currently a Ph.D. candidate in Centre for Sustainable Energy Technologies (CSET), University of Nottingham Ningbo China.

The second author is Professor Jo Darkwa, Director of CSET.

The third author is Dr Georgios Kokogiannakis

Correspondence:

Add: Centre for Sustainable Energy Technologies (CSET), University of Nottingham Ningbo China. 199 East Taikang Road, Ningbo 315100

Tel: +86 574 8818 0319

Fax: +86 574 8818 0313

Email: weiguang.su@nottingham.edu.cn

No designated Reviewers to be excluded.

Yours sincerely,

Weiguang Su

Review of solid-liquid phase change materials and their encapsulation technologies

Weiguang Su, Jo Darkwa, Georgios KOKOGIANNAKIS

Centre for Sustainable Energy Technologies, University of Nottingham Ningbo China

1 Introduction

Energy consumption in buildings continues to pose environmental problems to many countries and the world as a whole. Techniques such as thermal energy storage are being explored at different levels for reducing energy consumption in buildings which currently accounts for about 40% percentage of total global energy consumption [1]. Phase change materials (PCMs) are capable of storing and releasing large amounts of energy during melting and solidification at specific temperatures. Thermal energy storage does not only reduce the mismatch between energy supply and demand but also improves the performance and reliability of energy systems and plays an important role in conserving energy resources. Current application of PCMs in buildings include air conditioning i.e. free cooling [1], cold thermal storage media and absorption refrigeration. Other integrated systems are PCM Trombe wall, PCM wallboards, PCM shutter, PCM concrete, PCM under-floor heating systems, PCM ceiling boards[2-4] as well as hot water supply and waste heat recovery systems [5]. For instance, E.Oro *et al.* [6] and Gang Li *et al.*[7] reviewed PCMs melting point below 20 °C for cold thermal energy storage applications. Agyenim *et al.* [8] identified phase change materials of melting temperature within 0-65 °C to be suitable for domestic heating/cooling application. They also stated that PCMs of melting temperatures 80°C to 120°C could be used in absorption cooling system whereas those types of melting temperatures above 150°C could be applied in solar power plants systems coupled with parabolic trough collectors for direct steam generation. Furthermore, Cabeza *et al.* [9] stated more comprehensively that melting temperatures up to 21°C are more suitable for cooling applications, 22-28°C for thermal comfort applications, 29-60 °C for hot water supply and over 120°C for waste heat recovery applications.

Depending on the type of PCM, energy storage process could be described as solid-solid, solid-liquid, liquid-gas or solid-gas as shown in Fig. 1 [2, 3, 8, 9]. However, liquid-gas and solid-gas processes are not applicable to construction materials due to their large volume and pressure change during phase change process. On the other hand, solid-liquid types of organic PCMs could leak into their surroundings during heat storage process if they are applied directly without being encapsulated. Most of the organic PCMs also have low thermal conductivity and poor thermal response as well as being flammable which pose a serious potential danger of fire outbreak. Meanwhile, most inorganic PCMs are known to be corrosive which could cause irretrievable damage to storage containers [10]. These problems

1 may be overcome by employing encapsulation technology to produce enhanced
2 microencapsulated phase change material (MEPCM) or nanoencapsulated phase change
3 material (NEPCM) for various applications. As shown in Fig. 2, a typical structure of
4 MEPCM/NEPCM is composed of core and shell layers [11], which can be classified as
5 mononuclear, polynuclear or matrix type. This paper therefore focusses on review of various
6 types of solid-liquid PCMs and their related micro/nano-encapsulation technologies in order
7 to advance their development and application.
8
9

10
11
12 Figure 1 Classification of PCMs
13
14
15

16
17 Figure 2 Structure of MEPCMs/NEPCMs[11]
18
19

20 **2 Properties of solid-liquid PCMs**

21

22 There are a number of factors which can influence effectiveness and application of
23 solid-liquid types of PCMs. For instance good thermal properties depend on suitable phase
24 transition temperature, high latent heat of transition per unit weight, high thermal
25 conductivity, and large specific heat capacity. In the physical side PCMs should have
26 favourable phase equilibrium, high density, minor volume changes during phase transition,
27 and low vapour pressure at the operation temperature. For kinetic properties the PCMs need
28 to exhibit little or no sub-cooling during freezing, sufficient crystallization rate, melting and
29 solidification at the same temperature and phase segregation. They should also possess good
30 chemical properties capable of completing reversible freezing/melting cycle, long-term
31 chemical stability, compatibility with other materials, no degradation after long term thermal
32 cycles, non-corrosive, non-toxic, no fire hazard, and non-explosive compounds. These
33 properties are therefore reviewed in the following chapter for the different types of organic
34 and inorganic PCMs.
35
36
37
38
39
40

41 **2.1 Organic solid-liquid PCMs**

42

43 Organic solid-liquid PCMs are described as paraffin and non-paraffin materials (fatty acids,
44 alcohols and glycols). Organic materials have stable phase change temperature (without
45 phase segregation), consequent degradation of latent heat fusion, self-nucleation (no
46 supercooling) and usually non-corrosiveness[12].
47
48
49
50

51 **2.1.1 Paraffin materials**

52

53 Paraffin belongs to a family of saturated hydrocarbons with similar properties and molecular
54 formulas (C_nH_{2n+2}) with straight hydrocarbon chains. In general, the longer the length of
55 hydrocarbon chain (more carbon atoms in paraffin molecular formulas), the higher the
56
57
58
59

1 melting temperature. Paraffin materials are safe, reliable, predictable, less expensive,
2 non-corrosive and have low vapour pressure. However, they possess some undesirable
3 properties such as low thermal conductivity, non-compatible with the plastic container,
4 moderately flammable, a high volume change between the solid and liquid stages. Tab. 1
5 shows the thermophysical properties of the commercially available paraffin materials.
6

7
8 Table 1: Thermophysical properties of paraffin [2, 5, 9]
9

10 11 12 **2.1.2 Non-paraffin materials**

13
14 Non-paraffin organic materials such as esters, fatty acids, alcohols and glycols, can also be
15 used as PCMs as listed in Tab. 2. They are the largest group of candidate materials for latent
16 heat storage particularly, the fatty acids. They are however flammable and should therefore
17 not be exposed to excessively high temperature, flames or oxidizing agents. Other properties
18 of the non-paraffin PCMs include high heat of fusion, inflammability, low thermal
19 conductivity, low flash point, varying level of toxicity, and instability at high temperature.
20
21

22
23
24 Table 2: Thermophysical properties of non-paraffin PCMs [2, 5, 6, 9]
25
26
27

28 **2.2 Inorganic solid-liquid PCMs**

29 30 **2.2.1 Salt hydrates**

31
32 Salt hydrates in Tab.3 are the oldest and most studied PCMs, which can be regarded as alloys
33 of inorganic salts and water forming a typical crystalline solid of general formula $AB \cdot nH_2O$.
34 The solid-liquid transformation of salt hydrates is a dehydration of the salt, although this
35 process resembles melting or freezing thermodynamically. At the melting point the hydrate
36 crystals breakup into anhydrous salt and water, or into a lower hydrate and water, and the
37 melting behaviour of the salt hydrates can be identified as: congruent, incongruent and
38 semi-congruent melting[14]. Congruent melting occurs when the anhydrous salt is
39 completely soluble in its water of hydration at the melting temperature. Incongruent melting
40 occurs when the salt is not entirely soluble in its water of hydration at the melting point.
41 Semi-congruent melting occurs when the liquid and solid phases are in equilibrium during a
42 phase transition. The most attractive properties of salt hydrates are: (i) high latent heat of
43 fusion per unit volume, (ii) relatively high thermal conductivity (almost double of the
44 paraffin's), and (iii) small volume changes on melting. There is however supercooling and
45 phase segregation problems associated with their applications.
46
47
48
49
50
51
52
53

54 Table 3: Thermophysical properties of salt hydrates [2, 5, 9, 15]
55
56
57
58
59
60
61
62
63
64
65

2.2.2 Inorganic compounds

Tab. 4 shows a list of available inorganic compounds but some are considered to be unsuitable for application in buildings due to their relatively small latent heat capacity. In addition many of the inorganic PCM compounds are harmful to the environment and human health.

Table 4: Thermal physical properties of inorganic compounds[2, 5]

2.2.3 Metals

As shown in Table 5, low melting point metals and their alloys can be used as latent heat energy storage materials. These metals have high thermal conductivity, good electrical conductivity, low vapor pressure, low heat of fusion per unit weight but high heat of fusion per unit volume (due to large density), and small volume change during phase transition[17]. Thus, if certain metal or metal alloy is used as a PCM, the heat transfer capacity will be improved significantly compared with traditional PCMs. Therefore, low melting point liquid metals could be used for application in laser system[18], USB flash memory[19] and smartphone[20] cooling.

Table 5: Melting temperature and latent heat of metallic PCMs [2, 17]

2.3 Eutectics solid-liquid PCMs

Table 6 shows a list of Eutectic solid-liquid PCMs. They normally consist of two or more low melting temperature components, each of which melts and freezes congruently to form a mixture of the components' crystals during crystallization[2]. Eutectics do possess high thermal conductivity and density and do not experience any segregation and supercooling. However the latent and specific heat capacities are much smaller than salt hydrates and paraffin.

Table 6: Thermophysical properties of eutectic PCMs [2, 6, 9, 17]

2.4 Analysis of various PCMs

As highlighted in previous chapters, the advantages of organic solid-liquid PCMs include availability in a large temperature range, less super cooling, ability to melt congruently, self-nucleating, compatibility with conventional materials of construction, no segregation, chemical stable, high heat of fusion, safe and non-reactive and recyclable. They do however have disadvantages such as low thermal conductivity, low density and being flammable. On

1 the other hand, the inorganic solid-liquid PCMs have high density that means they have
2 higher heat storage capacity, they are cheaper and readily available, possess high thermal
3 conductivity and are non-flammable. Nevertheless, there are also some problems such as
4 supercooling and phase segregation associated with phase change process.
5

6 Fig. 3 illustrates the relationship between latent heat capacity of various PCMs and their
7 melting point temperatures. It shows that the organic, salt hydrate, eutectic and solid-solid
8 PCMs have relatively lower melting temperatures. The inorganic compound and metallic
9 PCMs have much higher melting temperature range but the metallic PCMs do in general
10 have the lowest latent energy storage capacity. Tables 1-5 indicate that only about 10% of
11 thermal conductivity (k) data for PCMs have been established over the past few years which
12 distributed in the range of 0.149-61 W/m·K. In order to highlight the difference of various
13 kinds of PCMs the relationship between the Log (k) and the melting temperatures is
14 presented in Fig. 4, and it is clear that the metallic and their compounds have much higher
15 thermal conductivities than the other inorganic PCMs and organic PCMs by over 10 W/m·K
16 (Log(k)>1). On the other hand, most of the inorganic PCMs have higher thermal conductivity
17 than the organic PCMs.
18
19
20
21
22
23
24

25 Figure 3 Melting temperature and latent heat distribution for different types of PCMs
26
27

28 Figure 4 Thermal conductivity distribution for different types of PCMs
29
30

31 **3 Development of micro/nano-encapsulated PCMs**

32
33
34
35

36 Microencapsulation is defined as a process in which tiny particles or droplets are surrounded
37 by a coating material, or embedded in a homogeneous or heterogeneous matrix, in order to
38 provide small capsules with useful properties[21]. Microencapsulation processes are usually
39 categorized into two groups: physical processes and chemical processes. Physical methods
40 include spray cooling, spray drying and fluidized bed processes. However, physical methods
41 are limited by their granulated sizes thus making them useful for producing micro
42 encapsulated PCM particles [22]. On the other hand, chemical methods can produce much
43 smaller encapsulated PCM particles. This chapter therefore reviews various types of
44 fabrication technologies for micro/nano-encapsulated PCMs (MEPCM/NEPCM).
45
46
47
48

49 **3.1 In-situ polymerization**

50
51

52 In-situ polymerization involves a process whereby chemical reaction takes place between
53 two immiscible liquids (water soluble phase and oil soluble phase) in a continuous phase,
54 such as emulsion, suspension, precipitation or dispersion polymerization and interfacial
55 polycondensations [11]. In general, the processes usually contains 4 steps: 1) Oil/water (O/W)
56
57
58
59

1 emulsion production, 2) preparation of prepolymer mixture liquid, 3) adding prepolymer
2 mixture liquid into O/W emulsion to encapsulate core material particles, 4) washing and
3 drying MEPCM/NEPCM. As an example, Fig. 5 shows the process of encapsulation of
4 n-octadecane with resorcinol-modified melamine–formaldehyde shell [23] using the in-situ
5 polymerization process.
6
7
8
9

10 Figure 5 Fabrication of the MEPCM by in-situ polymerization [23]

11 Choi *et al.* [24] used a melamine formaldehyde shell and 5 wt% styrene-maleic
12 anhydride-monomethyl (SMA) as emulsifier to encapsulate tetradecane. The result showed
13 reduction in the size of the capsules and uniformity was improved with an optimum
14 emulsion speed of up to 8000 rpm. Fang *et al.* [25] used a UF shell to encapsulate tetradecan
15 PCM. The liquid was emulsified at 60°C for 30min with an emulsion speed of 1500 rpm.
16 Sodium dodecyl sulfate and resorcin were used as emulsifier and system modifier
17 respectively. Further analysis of the results showed that the thermal stability of the capsules
18 was also improved after adding 2-5wt% of NaCl. Yang *et al.* [26] successfully fabricated four
19 types of MEPCM with different shell materials (PVAc, PS, PMMA and PEMA). Jin *et al.* [27]
20 dispersed paraffin using Hydrolyzed-styrene-alt-maleic anhydride(HSMA) as the emulsifier at
21 a speed of 12000 rpm and then used UF as a shell material to produce MEPCM. The content
22 of the shell material was then increased to 28% and was subjected to number of thermal
23 cycles. The results showed the capsules to be intact thus making them thermally stable than
24 a bulk paraffin material. Zhang *et al.*[28] encapsulated n-octadecane with MF material,
25 emulsifier (TA 0.6-2.3 wt%) and cyclohexane (0-36.8wt%) material. They observed that the
26 diameters of the microcapsules could be reduced by increasing the stirring speed from 3000
27 rpm to 9000 rpm. Li *et al.* [29] emulsified n-octadecane at a stirring rate of 8000 rpm and
28 then encapsulated it with MF shell to obtain MEPCM of an average diameter of 2.2µm and
29 latent heat capacity of 144kJ/kg. Hong and Park [30] fabricated MEPCM by using 53wt%
30 fragrant margin oil and MF as core and shell materials respectively. The experimental study
31 which was conducted at an emulsion speed of 3000 rpm resulted in a MEPCM of particle size
32 smaller than 10µm. Other encapsulation process involving binary mixture of n-hexadecane
33 and n-eicosane and MF as a shell material achieved a maximum energy storage capacity of
34 163-170kJ/kg [31]. Song *et al.* [32] also introduced nano-silver particles in in-situ
35 polymerization process to encapsulate bromo-hexadecane (BrC₁₆) with aminoplast as the
36 shell material. Their result did prove that nano-silver particles can enhance mechanical
37 strength and thermal stabilities of MEPCMs without experiencing any particle agglomeration
38 problem.
39
40
41
42
43
44
45
46
47
48
49
50

51 **3.1.1 Interfacial polycondensation**

52 Interfacial polycondensation is one of the in-situ processes wherein a microcapsule wall of a
53 polymer is formed at an interface between two phases with each of them containing a
54 suitable reaction monomer. Initially, a multifunctional monomer is dissolved in the organic
55
56
57
58
59

1 core material and then the resulting mixture is dispersed in an aqueous phase containing a
2 mixture of emulsifiers and protective colloid stabilizers. Combination of monomers is then
3 added to the aqueous phase for the formation of a polymer shell [33]. Fig. 6 shows a process
4 used by Zhang *et al.* [34] to synthesize microencapsulated n-octadecane with polyurea shells
5 which were produced with tolylene 2,4-diisocyanate (TDI) and three different amines namely,
6 ethylene diamine (EDA), diethylene triamine (DETA) and Jeffamine T403. The oil solution was
7 prepared by mixing together TDI and n-octadecane and then adding water to the mixture at
8 a stirring speed of 3000 rpm to produce O/W emulsion. Furthermore an EDA solution
9 consisting of 0.1wt % SMA was added into O/W emulsion at stirring rate of 600 rpm to
10 complete the interfacial polymerization process. The MEPCM produced with Jeffamine as the
11 amine monomer displayed the best anti-osmosis property.
12
13
14
15
16
17

18 Figure 6 Microcapsule manufactured by interfacial polycondensation [34]
19

20 Other studies have also been conducted using the same process. For instance, Chen *et al.* [35]
21 used butyl stearate as core material and TDI/EDA as shell material to produce MEPCM. They
22 also investigated the effect of different stirring rates (300-700 rpm), emulsifier (polyethylene
23 glycol octylphenyl ether (OP)-10) content and core/shell mass ratios on the quality of the
24 MEPCM. The results established a suitable stirring rate of 500 rpm for a core/shell mass ratio
25 of 4:1 but found no significant influence on the emulsifier. Zou *et al.*[36] also encapsulated
26 hexadecane with the same type of shell and emulsifier material as above but at a stirring
27 rate of 300rpm. Cho [37], Siddhan [38] and Su [39] all used TDI and DETA to produce shell
28 materials for encapsulating n-octadecane. The main difference between their methods was
29 that Siddhan and Su used higher stirring speed ranging from 2500-4000 rpm to produce the
30 O/W emulsion whereas Cho's emulsion speed was limited to a lower speed of 300 rpm.
31 Surprisingly, the average diameters of MEPCM particles produced by Siddhan and Su were
32 5 μ m and 7.3 μ m respectively as compared with 1 μ m obtained by Cho. Tseng *et al.* [40]
33 fabricated MEPCM of mean capsule diameter of 47-150 μ m by using 53-61wt% paraffins
34 (n-pentadecane, n-eicosane and paraffin wax) as core materials and UF for the shell.
35
36
37
38
39
40

41 In order to enhance thermal conductivities of organic MEPCMs other researchers have tried
42 the use of inorganic shell materials under the interfacial polycondensation encapsulation
43 process. Zhang *et al.* [41] used silicon dioxide (SiO₂) to encapsulate n-octadecane and
44 achieved thermal of about 0.6547 W/m·K. Pan et al. [42] used aluminium hydroxide (Al(OH)₃)
45 to encapsulate palmitic acid (PA) and obtained thermal conductivities ranging between
46 0.7-0.84 W/m·K. Li *et al.* [43] reported another development also based on silicon dioxide as
47 the shell and paraffin as the core material. The evaluation results showed that the capsules
48 were able to maintain stable phase transition without any sign of leakage after number of
49 repeated melting–freezing cycles.
50
51
52
53
54
55
56
57
58
59
60
61
62
63
64
65

3.1.2 Suspension polymerization

The use of suspension polymerization process for the fabrication of MEPCM usually follows certain basic procedures as: 1) Dissolution of polymer monomer into organic phase (core materials); 2) Production of oil/water (O/W) emulsion; 3) Separation and precipitation of the monomer molecules from core materials and generation of solid shell. Various researchers have produced MEPCMs using the suspension polymerization process. Fig. 7 describes the suspension polymerization process which Y.F. Ai *et al.* [44] used for microencapsulating n-hexadecane. The results demonstrated that higher emulsion speed could reduce particle sizes of MEPCMs.

Figure 7 Schematic of the fabrication MEPCM by suspension-like polymerization[44]

Sánchez *et al.* [45] fabricated MEPCMs by encapsulating 50wt% of paraffin wax PRS, tetradecane, Rubitherm 20 and nonadecane as core materials in a polystyrene shell. Further experimental studies by Sánchez *et al* [46] proved that crosslinking reaction temperature has no significant effect on the particle size distribution. It also revealed that it is difficult to achieve encapsulation when core/shell mass ratio is greater than 2.00. You *et al.* [47, 48] produced n-Octadecane microcapsules with a styrene (St)–divinylbenzene (DVB) copolymer shell and achieved an average diameter of 80µm and latent heat fusion capacity of 126kJ/kg. Thermogravimetric (TG) analysis of the St-DVB shell showed the initial weight-loss temperatures to be above 230 °C thus making it better than MF shell. Li *et al.*[49] microencapsulated n-octadecane with styrene-1,4-butylene glycol diacrylate copolymer (PSB), styrene–divinylbenzene copolymer (PSD), styrene-divinylbenzene-1,4-butylene glycol diacrylate copolymer (PSDB), and polydivinylbenzene (PDVB) shell materials. They then analysed the morphology of the MEPCMs from scanning electron microscope (SEM) images and found the type with PSDB shell to be the best of all the samples.

Much smaller MEPCM/NEPCM capsules have also been produced by microsuspension polymerization process. As shown in Fig. 8 [50] n-octadecane was encapsulated with a PDVB shell to obtain an average size of 1.5µm MEPCM. X. Qiu *et al.* [51] produced nanoencapsulated n-octadecane with different polymer shells (1,4-butylene glycol diacrylate (BDDA), divinyl benzene (DVB), trimethylol propane triacrylate (TMPTA) and pentaerythritol tetraacrylate (PETRA)). Their thermal properties, thermal resistant temperatures and shell mechanical strength of capsules were enhanced by increasing the level of cross-linking agents. Simultaneously, the cross-linking agent PETRA created the best NEPCM product which contained 75.3wt% core material with phase change enthalpy of 156.4-182.8kJ/kg and average particle diameter of 720nm. Cheng *et al.* [52] fabricated NEPCMs with a polyurethane shell and achieved a latent heat value of 104kJ/kg. The particle size was changed from 300 to 600 nm whilst the crosslinking agent tripropylene glycol diacrylate (TPGDA) increased from 10 wt% to 20 wt%.

1 Unlike other encapsulation technologies there is a special precautions must be taken under
2 some suspension polymerization processes. For instance when using polystyrene,
3 styrene-methyl methacrylate (St-MMA), polydivinylbenzene (PDVB) and polyurethane as
4 MEPCM shell materials nitrogen gas protection facility would be necessary during the
5 fabrication process and for the fact that the reaction time could take as long as 5-24 hours.
6
7
8
9

10 Figure 8 Schematic of the preparation of the PDVB/Octadecane capsules by the
11 microsuspension polymerization[50]
12

13 3.1.3 Emulsion/Miniemulsion polymerization 14 15

16 Emulsion polymerization takes place over a number of steps, where various chemical and
17 physical events take place simultaneously during the process of particle formation and
18 growth. Three major mechanisms for particle formation have been proposed to date. Particle
19 formation is considered to have taken place when (1) a free radical in the aqueous phase
20 enters a monomer-swollen emulsifier micelle and propagation proceeds therein or; (2) the
21 chain length of a free radical growing in the aqueous phase exceeds its solubility limit and
22 precipitates to form a particle nucleus, or; (3) a free radical growing in the aqueous phase
23 enters a monomer droplet and propagation proceeds therein [53].
24
25
26

27 Polymethylmethacrylate (PMMA) is a common shell material used for producing MEPCM
28 with emulsion polymerization method. For instance, Alkan *et al.* [54] encapsulated docosane
29 with PMMA for thermal energy storage material. The capsules contained 28wt% of core
30 material with a narrow particle size distribution (average particle size was 0.16 μm) and were
31 carefully controlled at emulsion stirring rate of 2000 rpm. Alkan *et al.* [55] further coated
32 PMMA shell material containing capsules of average diameter 0.70 μm with 35wt% of
33 n-Eicosane. Sari *et al.* [56, 57] also produced smaller sizes of NEPCM ranging from
34 0.14–0.40 μm with 43wt% of n-Octadecane and 38wt% n-Heptadecane as core materials
35 and at a stirring speed of 2000 rpm. Ma *et al.*[58] produced higher core material content
36 MEPCM which the core material content to be 61.2wt% and its latent heat capacity as much
37 as 101kJ/kg. During the polymerization process UV irradiation light intensity and exposure
38 time were used to control polymerization speed which helped to minimise the
39 polymerization time to only 30 minutes. SEM analysis revealed the diameter range of the
40 MEPCM as 0.5 to 2 μm . Alay *et al.* [59] developed n-hexadecane microcapsules for textile
41 application. The mean particle diameter of the capsules was in the range of 0.22 μm -1.05 μm
42 with corresponding enthalpy of 68.9-145.6kJ/kg.
43
44
45
46
47
48
49

50 Miniemulsion polymerization is the same process as emulsion polymerization, except that
51 smaller droplets can be produced as shown in Fig. 9. Homogenization can be achieved using
52 an ultrasonifier (for laboratory-scale batch process) or a high-pressure homogenizer (for
53 larger-scale processes). Luo and Zhou [60] used this method to develop nanoencapsulated
54 paraffin as thermal energy storage material. They however found out that the
55
56
57
58
59

1 thermodynamic factors (the level and type of surfactant and hydrophilic comonomer, and
2 the monomer/paraffin ratio), kinetic factors (the level of the crosslinking agent or
3 chain-transfer agent), and nucleation modes did have significant influence on the
4 encapsulation process. Chen *et al.* [61] produced nanocapsules of an average particle size of
5 150nm with n-Dodecanol as the core material and PMMA as the shell material. Maximum
6 phase change enthalpy of 98.8 J/g and encapsulation efficiency of 82.2% were obtained with
7 3% mass ratios of polymerizable emulsifier (DNS-86)/core material and 2% co-emulsifier
8 (hexadecane (HD))/core material. Li *et al.* [62] successfully synthesized NEPCM with the
9 two-step miniemulsion polymerization method and achieved a mean particle diameter of
10 270nm. The experimental results did reveal that by increasing the amount of surfactant
11 material (sodium dodecyl sulphate (SDS)) the phase-change enthalpy of the nanocapsules
12 did also increase but the mean particle size was reduced. Fuensanta *et al.* [63] encapsulated
13 paraffin wax (RT 80) of particle size ranging from 52-112 nm with encapsulation efficiency of
14 about 80%. Meanwhile, in comparison with raw RT80 its melting temperature was decreased
15 by 1–7°C but did show good thermal stability after 200 thermal cycles.
16
17
18
19
20
21
22

23 Figure 9 The procedure of miniemulsion polymerization[64]
24

25 **3.1.4 Concluding remark**

26 As summarised in Tab. 7, it is clear that various wax materials have been encapsulated with
27 different shell materials but melamine formaldehyde (MF), urea formaldehyde (UF),
28 polymethyl methacrylate (PMMA), polyurea and polystyrene appear to be the most widely
29 used shell materials due to their good chemical stability and mechanical strength. They
30 however, have low thermal conductivity and also some of the chemicals such as
31 formaldehyde can cause environmental and health problems during fabrication process of
32 the MEPCM/NEPCM. Although high thermal conductivity inorganic shells i.e. Al(OH)₃ and
33 SiO₂ have been used for thermal enhancement their presence did reduce the overall energy
34 storage capacities of the phase change materials.
35
36
37
38
39
40

41 Table 7: MEPCM/NEPCM fabricated by in-situ polymerization
42
43
44
45

46 **3.2 Complex coacervation**

47 Complex coacervation involves a reaction between two or more types of polymer materials
48 with oppositely charged crosslinks to copolymer shells. As shown in Fig. 10, the general
49 process consists of three stages carried out under continuous agitation as follows. 1) In the
50 first stage, coating material is dispersed in water to form a phase separation coacervation
51 and then a core material is added into the solution to produce O/W emulsion. 2) The second
52 stage involves adding another colloid solution charged with oppositely electric into the O/W
53 emulsion, and then adjusting the pH number of the solution appropriately. 3) The third stage
54
55
56
57
58
59

1 finishes it off with the cooling down of the mixture, microencapsulation and harvesting of
2 the MEPCM. The main limitation of this approach is the difficulty in scaling up the process
3 [67].
4
5
6

7 Figure 10 Flow diagram of a typical encapsulation process based on the complex
8 coacervation[67]
9

10 Nevertheless, a number of encapsulation developments have been carried out over the past
11 years with the complex coacervation method. Ozonur *et al.* [68] encapsulated natural
12 coco-fatty acid with gelatin–gum Arabic and achieved MEPCM of particle size of 1 mm. It was
13 subjected to a number of thermal cycles and found no physical deformation to its
14 geometrical shape. In comparison with pure coco-fatty, its melting temperature also
15 increased about 7°C. Onder *et al.*[69] used three types of paraffin waxes: n-hexadecane,
16 n-octadecane and n-nonadecane as core materials and gum arabic–gelatin mixture as a shell
17 material to produce MEPCMs. The results showed that microcapsules produced with
18 n-octadecane achieved the highest enthalpy value. They concluded that the quality of
19 MEPCM could be improved by ensuring precise pH value and correct amount of surfactants
20 at higher stirring rates. Hawlader *et al.*[70] established the optimal homogenizing time in
21 coacervation method as 10 minutes and the amount of cross-linking agent required as 6–8
22 ml. They also demonstrated that microencapsulation efficiency is dependent upon the
23 process parameters such as core material ratio, emulsifying time and the amount of
24 cross-linking agent. Bayes-Garcia [71] successfully produced Rubitherm® RT 27 microcapsules
25 from two different coacervates; Sterilized Gelatine/Arabic Gum for the SG/AG method and
26 Agar-Agar/Arabic Gum for the AA/AG method. According to the particle sizing analysis the
27 average diameter of the capsules produced with the SG/AG method was 12µm whereas the
28 AA/AG method achieved far smaller size of 104nm. Su *et al.* [72] also used the two-step
29 coacervation (TSC) method and an MF shell to encapsulate n-octadecane. This method
30 reduced the cracks on the shell and increased its compactness and permeability coefficient.
31
32
33
34
35
36
37
38
39

40 3.3 Sol-gel method

41 The term “sol-gel” is an abbreviation for “solution-gelling” and denotes a process by which
42 largely inorganic materials are synthesized. The process follows a principle whereby a
43 solution undergoes a transition to a gel characterized by an infinite three-dimensional
44 network structure spreading uniformly throughout the liquid medium [11]. For instance, H.
45 Zhang *et al.* [73] fabricated microcapsules of n-Octadecane with silica shell to enhance
46 thermal conductivity and phase-change performance, as shown in Fig. 11. The results
47 achieved good phase-change performance, high encapsulation efficiency, high thermal
48 conductivity and good antiosmosis property.
49
50
51
52
53
54
55
56

57 Figure 11 Schematic formation of a sol–gel process[73]
58
59
60
61
62
63
64
65

1 Other researchers have also fabricated MEPCMs using the sol-gel method but with silicon as
2 a shell material. Wang *et al.* [74] were the first to encapsulate PCMs with silicon and to
3 investigate the formation mechanism which established that the use of cationic surfactants
4 (i.e. cetyltrimethylammonium chloride, dodecyltrimethyl-ammonium chloride and
5 dodecyltrimethylammonium bromide) as emulsifiers are suitable for the production of
6 MEPCMs. Li *et al.* [75] prepared different composite MEPCMs based on paraffin/SiO₂/
7 expanded graphite and paraffin/SiO₂ and achieved much higher thermal conductivities than
8 pure paraffin. Fang *et al.*[76] also produced paraffin-based MEPCM using SiO₂ as a shell
9 material and reported solidification/melting temperatures of 57.02/58.37°C and latent heat
10 capacity of 107.05/165.68kJ/kg. Chang *et al.* [77] microencapsulated n-Octadecane using a
11 PMMA network-silica hybrid shell. They concluded that the most suitable condition for
12 producing high percentage (74%) of PCM microcapsules of high latent heat capacity
13 (180kJ/kg) was to add 5% of silicon dioxide (SiO₂) to the process. Chen *et al.* [78] produced
14 MEPCM (diameter 20–30µm) capsules by using 90.7 % of stearic acid (SA) and SiO₂ as core
15 and shell materials respectively. The experimental results achieved good thermal stability for
16 energy storage capacity of 162.0 - 171.0 kJ/kg over a phase change temperature range of
17 52.6°C-53.5°C. Chen *et al.*[79] further encapsulated high percentage (82.2%) content of
18 paraffin with SiO₂ shell and obtained good thermal characteristics. The results showed that
19 the microcapsules melted at 57.96°C (latent heat 156.86 kJ/kg) and solidified at 55.78°C
20 (latent heat 144.09 kJ/kg). Sara T.L. *et al.*[80] synthesized PCM nanocapsules which contained
21 palmitic acid (PA) as core and SiO₂ as shell materials. They observed that by progressively
22 increasing the pH level of the core material, the mean diameter and the energy storage
23 capacity of the nanocapsules also increased. For instance an increase in pH value from 11 to
24 12 resulted in an increase of 183.7 to 722.5 nm in the particle diameter and 168 to 181kJ/kg
25 in its energy storage capacity.

3.4 Solvent extraction/evaporation method

37 Inorganic PCMs can be encapsulated by solvent extraction/evaporation method through the:
38 (i) incorporation of the bioactive compound, (ii) formation of the microdroplets, (iii) solvent
39 removal and (iv) harvesting and drying the particles. As shown in Fig. 12, Salaün *et al.* [81]
40 studied sodium phosphate dodecahydrate (DSP, Na₂HPO₄·12H₂O) encapsulation by solvent
41 evaporation–precipitation method with various organic solvents and cellulose acetate
42 butyrate (CAB) crosslinked by methylene diisocyanate (MDI). It was evident in the results
43 that surface appearance of MEPCM depends on the rate of polymer precipitation at the
44 interface, and that thermal stability and the thermal degradation were strongly influenced by
45 the core content and the surface roughness of the MEPCM.

46 Figure 12 Schematic overview of microencapsulation by solvent extraction/evaporation
47 method[81]

1 In other studies, Wang and Huang [82] encapsulated DSP with PMMA using the same
2 method and was able to produce uniform sizes of 1–10µm MEPCM capsules within
3 polymerization time of 4 hours at a reaction temperature of 80-90°C. The maximum
4 measured energy storage capacity was obtained as 173.9 kJ/kg at a temperature of 51°C.
5 Wang *et al.* [83] recently encapsulated DSP with PMMA and UF. They obtained mean MEPCM
6 diameters of 6µm and 500nm with corresponding latent heat capacity of 142.90kJ/kg and
7 121.20kJ/kg. However, the encapsulation efficiencies of UF and PMMA shell were only 55.74%
8 and 63.97% respectively and also noticed that and the organic solvent residual in MEPCM
9 could cause the leakage problem after few multiple heating-cooling cycles. Huang *et al.*[84]
10 further encapsulated a hydrated salt (Na₂HPO₄·7H₂O) as phase change energy storage
11 material by modifying PMMA. The morphology study revealed the mean diameter of the
12 capsules to be about 6.8µm. The thermal analysis showed that the weight loss in the MEPCM
13 was less than 10% during the heating process from 30 to 84 °C. The phase change melting
14 point was 51°C whereas the heat of fusion was obtained as 150kJ/kg.
15
16
17
18
19
20

21 **3.5 Other micro-/nano-encapsulation methods**

22
23 Apart from the already discussed encapsulation technologies, other technologies such as
24 phase separation method, internal phase separation method, pre-polymer mixing method
25 and self-assembling method do exist. For instance, Loxley and Vincent [85] proposed phase
26 separation method to encapsulate n-Hexadecane with polymethylmethacrylate (PMMA). The
27 encapsulation process as shown in Fig. 13 involves: (1) preparation of PMMA and dissolving
28 PMMA in dichloromethane and then adding hexadecane, (2) stirring emulsion at a speed of
29 10,000 rpm to produce oil droplets (3) migration of polymer-rich phase on core material
30 particles surface, 4) removal all of volatile solvent to finish off encapsulation. Yang *et al.* [86]
31 used the phase separation method to produce microencapsulated n-tetradecane with
32 different shell materials (Acrylonitrile–styrene copolymer (AS),
33 acrylonitrile–styrene–butadiene copolymer (ABS) and polycarbonate (PC)). The particle sizes
34 were less than 1µm with melting enthalpy of more than 100 kJ/kg and encapsulation
35 efficiency of 66–75%for all the three shell materials.
36
37
38
39
40
41
42
43

44 Figure 13 Schematic of the encapsulation process[85]

45 (n.v.n.s. - non-volatile non-solvent; v.s.- volatile solvent)

46
47
48 Jiang *et al.* [87] produced microcapsules with phenolic resin (PFR) shell and n-hexadecane
49 core by internal phase separation method. The microcapsules exhibited smooth and perfect
50 structure but the melting point temperature did slightly reduce in comparison with pure
51 n-hexadecane and also supercooling was observed upon crystallization. Zhang *et al.*[88]
52 produced 1-2µm diameter encapsulated n-tetradecane with PMMA and polystyrene (PS)
53 using the same method. The results indicated that optimal microcapsules could be produced
54 with a core/shell ratio of 3:1 and achieve a latent heat capacity of 151kJ/kg.
55
56
57
58
59

1 Through the pre-polymer mixing process, Kim E.Y. and Kim H.D. [89] encapsulated
2 n-octadecane with waterborne polyurethane (WBPU) shell to obtain microcapsules of sizes
3 ranging from 1-6 μ m. The results showed the sizes to be reducing with increasing amount
4 of emulsifier. The heat of fusion, heat of crystallization, and encapsulation efficiencies of
5 n-octadecane were also found to increase with increasing amount of microencapsulated
6 blends, thickener and hardener.
7

8
9 Fig. 14 shows the self-assembling procedure which was recently used by Yu *et al.* [90] to
10 encapsulate n-octadecane with calcium carbonate (CaCO₃) as a shell material. Different
11 core/mass ratios of 30/70, 40/60 and 50/50 were used for the fabrication to obtain
12 corresponding energy storage capacities of 46.93 kJ/kg, 67.91 kJ/kg and 84.37 kJ/kg. Thermal
13 conductivities ranging from 1.264-1.674 W/m·K were obtained but more than 60% of the
14 n-octadecane was wasted during the encapsulation process due to low encapsulation
15 efficiency.
16
17
18
19
20

21 Figure 14 Scheme of MEPCM formation with CaCO₃ shell via a self-assembly method [90]
22
23

24 **3.6 Comparison of various microencapsulation technologies**

25
26 The review has shown that micro/nano organic PCMs can be encapsulated by various
27 methods such as in-situ polymerization which include: interfacial polycondensation,
28 suspension polymerization and emulsion/miniemulsion polymerization, complex
29 coacervation, and sol-gel methods etc. In brief, in-situ suspension polymerization and
30 complex coacervation method can be used to produce large particle size MEPCMs with high
31 core material content and encapsulation efficiency. In-situ emulsion/miniemulsion
32 polymerization methods are suitable for producing nanocapsules. However, in-situ
33 suspension-like and in-situ emulsion/miniemulsion polymerization methods are hardly
34 applied to large scale production. This is due to the fact that high stirring rate is needed to
35 generate oil droplets during encapsulation process which in turn results in high energy
36 consumption and production costs. For instance, the emulsion speed used for in the
37 reviewed in-situ polymerization encapsulation processes was found to be in the range of
38 1000 to 13500 rpm depending on the particle size. In contrast, the polymerization reaction
39 process was achieved with a relatively lower stirring speed of 300-600 rpm. Regarding the
40 other processes covering sol-gel, in-situ polymerization and self-assembling methods, they
41 can all be used to encapsulate organic PCMs using inorganic shells in order to produce
42 MEPCM with high thermal conductivity and good fire resistance. However, inorganic shells
43 have poor mechanical strength and are not as flexible as copolymers which could impact on
44 the life cycle of the MEPCM.
45
46
47
48
49
50
51
52

53 In contrast encapsulation of micro/nano inorganic PCMs are limited to only solvent
54 extraction/evaporation method. Microencapsulated inorganic PCMs are more expensive
55 than organic PCMs due to the large amount of non-volatile organic solvents (i.e. toluene,
56
57
58
59
60
61
62
63
64
65

1 carbon tetrachloride, chloroform and acetone) which are employed within the solvent
2 extraction/evaporation encapsulation process. Beside this the residual organic solvent in
3 MEPCM could permeate the shell materials (e.g. UF, PMMA, CAB-MDI etc.) and cause
4 leakage problem after a period of thermal cycling. In general the encapsulation processes
5 have shown that the higher the emulsion speed the smaller the sizes of the capsules.
6 Meanwhile microencapsulation efficiencies do decrease as the ratios of core-to-coating
7 increase. See as the summarized data in Tab. 8.
8
9

10 Table 8: Statistics results of MEPCM/NEPCM via various encapsulation technologies
11
12
13

14 The review has also highlighted that crosslinking takes the longest period in the whole
15 microencapsulation process usually 2-5 hours, but could take as long 24 hours for silicon
16 based shells. Apart from the crosslinking time most shell monomers require additional and
17 external heating period to finish off copolymerization while gelatin-gum Arabic materials
18 need to be cooled down to about 5-10°C. Meanwhile all the major manufacturers of these
19 microencapsulation shell materials have cautioned that these materials could be harmful to
20 human and the environment. There is therefore the need for the dosage of the materials to
21 be optimized in order to achieve complete reaction and to neutralise any unreacted reagents
22 after crosslinking.
23
24
25
26
27

28 **4 Evaluation of MEPCM/NEPCM**

29
30

31 There are many standard instruments and methods for evaluating the properties of
32 MEPCM/NEPCM capsules. For instance, differential scanning calorimetry (DSC) [91] can be
33 used to measure the phase change latent enthalpy and phase change temperature; thermal
34 gravimetric analysis (TGA) can be used the measurement of thermal stability. Thermal
35 conductivities can be obtained with instruments such as laser thermal
36 diffusivity-conductivity instrument (Germany, NETZSCH, LFA447) [83], Thermal Property
37 Analyzer (USA, Decagon Devices, KD2 Pro) [92], EKO HC-110 thermal conductivity tester [73],
38 and thermal conductivity apparatus (Cussons Technology) [93]. Various microscopes (i.e.
39 scanning electron microscopy (SEM), transmission electron microscope (TEM) and optical
40 microscope) and dynamic light scattering particle size analyser could be used to study the
41 particle size distribution and morphology of MEPCM/NEPCM. Fourier transform infrared
42 (FT-IR) spectroscopy and X-ray diffraction (XRD) methods are also available for analysing the
43 chemical structure of MEPCM/NEPCM shell materials. Apart from these technologies, other
44 methods have been improved or developed for evaluating the properties of MEPCM/NEPCM.
45
46
47
48
49
50
51

52 **4.1 Thermal energy storage capacity and phase change temperature**

53

54 As an improvement on the traditional DSC equipment, Wang *et al.* [94] used an optical DSC
55 system to record and analyse the thermal properties of different composite PCMs before and
56
57
58
59

1 after their phase change processes. They reported high measurement accuracy of phase
2 change temperatures and enthalpies of less than 5% in comparison with the theoretical
3 values.

4
5 In order to determine latent heat and melting temperature of larger samples, Zhang *et al.*
6 [95] developed the T-history method. Eva Günther *et al.* [96] compared the T-history method
7 with two types of DSC measurement modes: dynamic mode and isothermal step mode. They
8 found out that the isothermal step mode offers higher precision than dynamic mode, but the
9 T-history method is more suitable for heterogeneous PCMs. Desgrosseilliers *et al.* [97] has
10 since then improved on the T-history enthalpy model and been successfully used for
11 evaluating composition-dependent two-phase equilibrium processes.

12
13 Besides evaluate MEPCM/NEPCM thermal energy storage capacity, latent heats
14 measurement results can be used to calculate the core material content ratio in
15 MEPCM/NEPCM by compare the thermal energy storage capacity with pure PCMs.
16 Meanwhile, Tseng *et al.* [40] assumed the MEPCM particle was a perfect sphere and then
17 through core material content and MEPCM diameter to calculate the shell thickness.
18 Moreover, it's helpful for evaluation of micro/nano-encapsulation process, i.e.: Zhang *et al.*
19 [34] suggested using encapsulation efficiency which was defined as the ratio of the actual
20 core content of the microcapsules to the theoretical core content.

27 **4.2 Thermal conductivity**

28
29 For the evaluation of thermal conductivity of NEPMC/MEPCM, researchers such as Meng and
30 Wang [98], Wang *et al.* [99] and Hunger *et al.* [100] have built and tested other devices using
31 the hot wire method. Meanwhile, the effective thermal conductivities of MECPMs and their
32 compositions have been studied with various methods. Zhao *et al.* [101] used the 3ω
33 method [102] in an experimental study and achieved the maximum effective thermal
34 conductivity of the MEPCM at its peak value of the phase change temperature. They also
35 observed that the conductivity value did increase as the density of the material was
36 increased. This was attributed to reduction in the porosity of the MEPCM. Darkwa and Kim
37 [103] developed an effective thermal conductivity testing rig in accordance with ISO 8301
38 Standards and used it to determine the thermal conductivity of a composite MEPCM sample
39 as shown in Fig. 15. Similarly, Marchi *et al.* [104] tested the thermal conductivity of panels
40 containing MEPCM by using the thermofluximeter method and in accordance with the
41 EN12667:2001 Standards. The experimental results were closely in agreement with the
42 theoretical predictions based on the effective medium theory (EMT) equations.

43
44
45
46
47
48
49
50
51
52
53
54
55
56
57
58
59
60
61
62
63
64
65
Figure 15 Thermal conductivity testing rig

54 **4.3 Thermal stability**

57 Thermal stability of MECPMs is an important property to ensure long term usage. Hong and

1 Park [30] investigated the long term stability of MEPCM under a 60- day drying experimental
2 test. As shown in Fig. 16 a known weight sample of MEPCM was dried under 25°C and 60°C
3 respectively, and weighed after every 10 days for the resident weight percentage. The results
4 show that the progressive residual weight percentage at 60°C drying condition was about 42%
5 whereas under 25°C it was at the rate of 8% after 60 days. Sharma *et al.* [105] proposed an
6 accelerated thermal cycle testing method to study the changes in latent heat and melting
7 temperature of acetamide, stearic acid and paraffin wax. The results showed good thermal
8 stability for the paraffin and acetamide after 1500 thermal cycles. Alkan *et al.* [54] also
9 performed series of thermal stability tests on PMMA/docosane microcapsules using their
10 DSC curves and FT-IR data and found no significant changes in their phase change
11 temperatures, latent heat enthalpies and chemical structures after number of thermal
12 cycles.
13
14
15
16
17
18

19 Figure 16 Resident weight (%) of melamine resin microcapsules in long self-life test[30]
20
21

22 **4.4 Mechanical strength**

23

24 Zhang *et al.*[106], Sun and Zhang [107, 108] and Hu *et al.* [109] have all through the
25 micromanipulation technology (shown in Fig. 17) determined the mechanical properties of
26 various MEPCMs/NEPCMs. It involves using a single probe in squeezing a microcapsule which
27 is positioned on a slide and then measuring its bursting strength. The probe is connected to a
28 force transducer and mounted on a 3D micromanipulator that can be programmed to travel
29 at a given speed. The slide is placed on the stage of an inverted microscope. When a
30 microcapsule is squeezed, the force being imposed on it is measured simultaneously by
31 sampling the voltage signal from the force transducer. When the probe eventually touches
32 the slide, the force will increase rapidly to signal the end of the test as displayed in Fig. 18.
33 Sun and Zhang's investigation [107] showed that the mean bursting force and yield point did
34 not change significantly with different compression speed.
35
36
37
38
39
40
41

42 Figure 17 Schematic diagram of the micromanipulation rig[107]
43
44
45

46 Figure 18 Force versus probe moving distance [107]
47

48 Su *et al.* [110] studied the mechanical properties of microcapsules covered with M/F shells
49 by using their SEM photographs and different compression loads. They concluded that when
50 the mass ratio of the core and shell material was 3:1, a yield point of was achieved with a
51 compression load of about 1.1×10^5 Pa. They also reported that the microcapsules displayed
52 a form of plastic behaviour when the compression load was increased beyond that point. The
53 double shells were however found to possess better mechanical properties. Darkwa *et al.* [92]
54 also investigated mechanical strength of bulk of microcapsules with similar method and
55
56
57
58
59

1 found no sign of fragmentation of the MEPCM particles after a pressure of 2.8MPa was
2 applied.
3

4 **4.5 Chemical stability**

5

6 Anti-Osmosis test is an important approach for determining the rate of weight loss and thus
7 chemical stability of MEPCMs. Zhang *et al.* [34] used this method for evaluating the
8 durability of samples of MEPCMs. The releasing rate (weight percentage of the released
9 substance) of 10 g of microencapsulated n-octadecane was measured by dispersing it in a
10 50ml acetone (as an extraction solvent) and at a stirring speed of 200 rpm. Analysis of the
11 results showed that the release rate of the microcapsules increased when the weight
12 percentage of the core materials increased and that the shell produced with Jeffamine
13 material exhibited the best anti-osmosis behaviour. Zhang *et al.* [73] capitalised on this
14 findings and evaluated SiO₂ coated n-octadecane with the same method. Su *et al.* [39] also
15 used this method but with different extraction solvent (ethyl alcohol) to evaluate another
16 type of MEPCM. The however found out that the amount of emulsifier used in that
17 investigation had some effect on the material's anti-osmosis property.
18
19
20
21
22
23

24 **5 Conclusions**

25

26 This paper was focused on the review of various types of organic and inorganic solid-liquid
27 PCMs and their thermophysical properties for various energy storage applications. The
28 review has shown that organic solid-liquid PCMs have more advantages in terms of wider
29 temperature range application, less super cooling and segregation effects, and other
30 capabilities. They do however have disadvantages such as low thermal conductivity, low
31 density and being flammable. In contrast, inorganic solid-liquid PCMs possess higher heat
32 storage capacities and conductivities, cheaper and readily available as well as being
33 non-flammable. Nevertheless in-organic PCMs do experience problems associated with
34 supercooling and phase segregation during phase change process.
35
36
37
38
39
40

41 The paper also examined the technologies being employed for encapsulation of PCMs and
42 the limitations of some of encapsulation shell materials. For instance some inorganic shells
43 are good for encapsulation and thermal conductivity enhancement of PCMs but do
44 experience low encapsulation efficiency, longer crosslinking time and low mechanical
45 strength. It was however identified that thermal and chemical stability and the mechanical
46 strength of encapsulated PCMs could strongly be influenced by the morphology of their
47 particles. Further development towards the enhancement of these properties is therefore
48 encouraged. Regarding evaluation methods, there are number of standalone systems which
49 have proved to be reliable but may require some form of standardisation especially in the
50 area of evaluation of mechanical properties.
51
52
53
54
55
56
57
58
59
60
61
62
63
64
65

References

- [1] Waqas A, Ud Din Z. Phase change material (PCM) storage for free cooling of buildings—A review. *Renewable and Sustainable Energy Reviews*. 2013;18:607-25.
- [2] Sharma A, Tyagi VV, Chen CR, Buddhi D. Review on thermal energy storage with phase change materials and applications. *Renewable and Sustainable Energy Reviews*. 2009;13:318-45.
- [3] Zhou D, Zhao CY, Tian Y. Review on thermal energy storage with phase change materials (PCMs) in building applications. *Applied Energy*. 2012;92:593-605.
- [4] Baetens R, Jelle BP, Gustavsen A. Phase change materials for building applications: A state-of-the-art review. *Energy and Buildings*. 2010;42:1361-8.
- [5] Sharma SD, Kitano H, Sagara K. Phase change materials for low temperature solar thermal applications. *Res Rep Fac Eng Mie Univ*. 2004;29:31-64.
- [6] Oró E, de Gracia A, Castell A, Farid MM, Cabeza LF. Review on phase change materials (PCMs) for cold thermal energy storage applications. *Applied Energy*. 2012;99:513-33.
- [7] Li G, Hwang Y, Radermacher R. Review of cold storage materials for air conditioning application. *International Journal of Refrigeration*. 2012;35:2053-77.
- [8] Agyenim F, Hewitt N, Eames P, Smyth M. A review of materials, heat transfer and phase change problem formulation for latent heat thermal energy storage systems (LHTESS). *Renewable and Sustainable Energy Reviews*. 2010;14:615-28.
- [9] Cabeza LF, Castell A, Barreneche C, de Gracia A, Fernández AI. Materials used as PCM in thermal energy storage in buildings: A review. *Renewable and Sustainable Energy Reviews*. 2011;15:1675-95.
- [10] Zhao CY, Zhang GH. Review on microencapsulated phase change materials (MEPCMs): Fabrication, characterization and applications. *Renewable and Sustainable Energy Reviews*. 2011;15:3813-32.
- [11] Ghosh SK. Functional coatings : by polymer microencapsulation. Swapan Kumar Ghosh 2006.
- [12] Kuznik F, David D, Johannes K, Roux J-J. A review on phase change materials integrated in building walls. *Renewable and Sustainable Energy Reviews*. 2011;15:379-91.
- [13] Parameshwaran R, Kalaiselvam S. Energy efficient hybrid nanocomposite-based cool thermal storage air conditioning system for sustainable buildings. *Energy*. 2013.
- [14] Sharma SD, Sagara K. Latent Heat Storage Materials and Systems: A Review. *International Journal of Green Energy*. 2005;2:1-56.
- [15] Farid MM, Khudhair AM, Razack SAK, Al-Hallaj S. A review on phase change energy storage: materials and applications. *Energy Conversion and Management*. 2004;45:1597-615.
- [16] Turnbull AG. Thermal Conductivity of Phosphoric Acid. *Journal of Chemical & Engineering Data*. 1965;10:118-9.
- [17] Ge H, Li H, Mei S, Liu J. Low melting point liquid metal as a new class of phase change material: An emerging frontier in energy area. *Renewable and Sustainable Energy Reviews*. 2013;21:331-46.

- 1 [18] Chi W, Guo J, Zhou X, Ren X. Experimental research and application analysis of solid-to-liquid
2 phase-change material. *Qiangjiguang Yu Lizishu/High Power Laser and Particle Beams*.
3 2009;21:1170-4.
- 4 [19] Ge H, Liu J. Phase change effect of low melting point metal for an automatic cooling of USB
5 flash memory. *Frontiers in Energy*. 2012;6:207-9.
- 6 [20] Ge H, Liu J. Keeping Smartphones Cool With Gallium Phase Change Material. *Journal of Heat*
7 *Transfer*. 2013;135:1-5.
- 8 [21] POSHADRI A, KUNA A. MICROENCAPSULATION TECHNOLOGY: A REVIEW. *JRes ANGRAU*.
9 2010;38:86-102.
- 10 [22] Smith MC. Microencapsulated phase change materials for thermal energy storage. New
11 Zealand: The University of Auckland; 2009.
- 12 [23] Zhang H, Wang X. Fabrication and performances of microencapsulated phase change
13 materials based on n-octadecane core and resorcinol-modified melamine-formaldehyde shell.
14 *Colloids and Surfaces A: Physicochemical and Engineering Aspects*. 2009;332:129-38.
- 15 [24] Choi JK, Lee JG, Kim JH, Yang HS. Preparation of microcapsules containing phase change
16 materials as heat transfer media by in-situ polymerization. *Journal of Industrial and Engineering*
17 *Chemistry*. 2001;7:358-62.
- 18 [25] Fang G, Li H, Yang F, Liu X, Wu S. Preparation and characterization of nano-encapsulated
19 n-tetradecane as phase change material for thermal energy storage. *Chemical Engineering*
20 *Journal*. 2009;153:217-21.
- 21 [26] Yang R, Xu H, Zhang Y. Preparation, physical property and thermal physical property of
22 phase change microcapsule slurry and phase change emulsion. *Solar Energy Materials and Solar*
23 *Cells*. 2003;80:405-16.
- 24 [27] Jin Z, Wang Y, Liu J, Yang Z. Synthesis and properties of paraffin capsules as phase change
25 materials. *Polymer*. 2008;49:2903-10.
- 26 [28] Zhang XX, Fan YF, Tao XM, Yick KL. Fabrication and properties of microcapsules and
27 nanocapsules containing n-octadecane. *Materials Chemistry and Physics*. 2004;88:300-7.
- 28 [29] Li W, Zhang X-X, Wang X-C, Niu J-J. Preparation and characterization of microencapsulated
29 phase change material with low remnant formaldehyde content. *Materials Chemistry and Physics*.
30 2007;106:437-42.
- 31 [30] Hong K, Park S. Melamine resin microcapsules containing fragrant oil: synthesis and
32 characterization. *Materials Chemistry and Physics*. 1999;58:128-31.
- 33 [31] Salaün F, Devaux E, Bourbigot S, Rumeau P. Development of phase change materials in
34 clothing part I: Formulation of microencapsulated phase change. *Textile Research Journal*.
35 2010;80:195-205.
- 36 [32] Song Q, Li Y, Xing J, Hu JY, Marcus Y. Thermal stability of composite phase change material
37 microcapsules incorporated with silver nano-particles. *Polymer*. 2007;48:3317-23.
- 38 [33] Sarier N, Onder E. Organic phase change materials and their textile applications: An
39 overview. *Thermochimica Acta*. 2012;540:7-60.
- 40 [34] Zhang H, Wang X. Synthesis and properties of microencapsulated n-octadecane with
41 polyurea shells containing different soft segments for heat energy storage and thermal regulation.
42 *Solar Energy Materials and Solar Cells*. 2009;93:1366-76.
- 43
44
45
46
47
48
49
50
51
52
53
54
55
56
57
58
59
60
61
62
63
64
65

- 1 [35] Liang C, Lingling X, Hongbo S, Zhibin Z. Microencapsulation of butyl stearate as a phase
2 change material by interfacial polycondensation in a polyurea system. *Energy Conversion and*
3 *Management*. 2009;50:723-9.
- 4 [36] Zou GL, Tan ZC, Lan XZ, Sun LX, Zhang T. Preparation and characterization of
5 microencapsulated hexadecane used for thermal energy storage. *Chinese Chemical Letters*.
6 2004;15:729-32.
- 7 [37] Cho JS, Kwon A, Cho CG. Microencapsulation of octadecane as a phase-change material by
8 interfacial polymerization in an emulsion system. *Colloid and Polymer Science*. 2002;280:260-6.
- 9 [38] Siddhan P, Jassal M, Agrawal AK. Core content and stability of n-octadecane-containing
10 polyurea microcapsules produced by interfacial polymerization. *Journal of Applied Polymer*
11 *Science*. 2007;106:786-92.
- 12 [39] Su J-F, Wang L-X, Ren L. Synthesis of polyurethane microPCMs containing n-octadecane by
13 interfacial polycondensation: Influence of styrene-maleic anhydride as a surfactant. *Colloids and*
14 *Surfaces A: Physicochemical and Engineering Aspects*. 2007;299:268-75.
- 15 [40] Tseng YH, Fang MH, Tsai PS, Yang YM. Preparation of microencapsulated phase-change
16 materials (MCPCMs) by means of interfacial polycondensation. *Journal of Microencapsulation*.
17 2005;22:37-46.
- 18 [41] Zhang H, Sun S, Wang X, Wu D. Fabrication of microencapsulated phase change materials
19 based on n-octadecane core and silica shell through interfacial polycondensation. *Colloids and*
20 *Surfaces A: Physicochemical and Engineering Aspects*. 2011;389:104-17.
- 21 [42] Pan L, Tao Q, Zhang S, Wang S, Zhang J, Wang S, et al. Preparation, characterization and
22 thermal properties of micro-encapsulated phase change materials. *Solar Energy Materials and*
23 *Solar Cells*. 2012;98:66-70.
- 24 [43] Li B, Liu T, Hu L, Wang Y, Gao L. Fabrication and Properties of Microencapsulated
25 Paraffin@SiO₂ Phase Change Composite for Thermal Energy Storage. *ACS Sustainable Chemistry*
26 *& Engineering*. 2013;1:374-80.
- 27 [44] Y.F. Ai Y], J. Sun, D.Q. Wei. Microencapsulation of n-hexadecane as phase change material by
28 suspension polymerization. *e-Polymers*. 2007;9:pp. 1-98.
- 29 [45] Sánchez L, Sánchez P, de Lucas A, Carmona M, Rodríguez JF. Microencapsulation of PCMs
30 with a polystyrene shell. *Colloid and Polymer Science*. 2007;285:1377-85.
- 31 [46] Sánchez L, Sánchez P, Carmona M, Lucas A, Rodríguez J. Influence of operation conditions on
32 the microencapsulation of PCMs by means of suspension-like polymerization. *Colloid and*
33 *Polymer Science*. 2008;286:1019-27.
- 34 [47] You M, Zhang X, Wang J, Wang X. Polyurethane foam containing microencapsulated
35 phase-change materials with styrene-divinylbenzene co-polymer shells. *Journal of Materials*
36 *Science*. 2009;44:3141-7.
- 37 [48] You M, Wang X, Zhang X, Zhang L, Wang J. Microencapsulated n-Octadecane with
38 styrene-divinylbenzene co-polymer shells. *Journal of Polymer Research*. 2011;18:49-58.
- 39 [49] Li W, Song G, Tang G, Chu X, Ma S, Liu C. Morphology, structure and thermal stability of
40 microencapsulated phase change material with copolymer shell. *Energy*. 2011;36:785-91.
- 41
42
43
44
45
46
47
48
49
50
51
52
53
54
55
56
57
58
59
60
61
62
63
64
65

- 1 [50] Chaiyasat P, Chaiyasat A. Preparation of poly(divinylbenzene) microencapsulated
2 octadecane by microsuspension polymerization: Oil droplets generated by phase inversion
3 emulsification. *RSC Advances*. 2013.
- 4 [51] Qiu X, Li W, Song G, Chu X, Tang G. Fabrication and characterization of microencapsulated
5 n-octadecane with different crosslinked methylmethacrylate-based polymer shells. *Solar Energy*
6 *Materials and Solar Cells*. 2012;98:283-93.
- 7 [52] Cheng F, Wei Y, Zhang Y, Wang F, Shen T, Zong C. Preparation and characterization of
8 phase-change material nanocapsules with amphiphilic polyurethane synthesized by
9 3-allyloxy-1,2-propanediol. *Journal of Applied Polymer Science*. 2013:n/a-n/a.
- 10 [53] Nomura M, Tobita H, Suzuki K. Emulsion Polymerization: Kinetic and Mechanistic Aspects. In:
11 Okubo M, editor. *Polymer Particles*: Springer Berlin Heidelberg; 2005. p. 1-128.
- 12 [54] Alkan C, Sarı A, Karaipekli A, Uzun O. Preparation, characterization, and thermal properties
13 of microencapsulated phase change material for thermal energy storage. *Solar Energy Materials*
14 *and Solar Cells*. 2009;93:143-7.
- 15 [55] Alkan C, Sarı A, Karaipekli A. Preparation, thermal properties and thermal reliability of
16 microencapsulated n-eicosane as novel phase change material for thermal energy storage.
17 *Energy Conversion and Management*. 2011;52:687-92.
- 18 [56] Sarı A, Alkan C, Karaipekli A. Preparation, characterization and thermal properties of
19 PMMA/n-heptadecane microcapsules as novel solid-liquid microPCM for thermal energy storage.
20 *Applied Energy*. 2010;87:1529-34.
- 21 [57] Sarı A, Alkan C, Karaipekli A, Uzun O. Microencapsulated n-octacosane as phase change
22 material for thermal energy storage. *Solar Energy*. 2009;83:1757-63.
- 23 [58] Ma S, Song G, Li W, Fan P, Tang G. UV irradiation-initiated MMA polymerization to prepare
24 microcapsules containing phase change paraffin. *Solar Energy Materials and Solar Cells*.
25 2010;94:1643-7.
- 26 [59] Alay S, Alkan C, Göde F. Synthesis and characterization of poly(methyl
27 methacrylate)/n-hexadecane microcapsules using different cross-linkers and their application to
28 some fabrics. *Thermochimica Acta*. 2011;518:1-8.
- 29 [60] Luo Y, Zhou X. Nanoencapsulation of a hydrophobic compound by a miniemulsion
30 polymerization process. *Journal of Polymer Science Part A: Polymer Chemistry*.
31 2004;42:2145-54.
- 32 [61] Chen Z-H, Yu F, Zeng X-R, Zhang Z-G. Preparation, characterization and thermal properties of
33 nanocapsules containing phase change material n-dodecanol by miniemulsion polymerization
34 with polymerizable emulsifier. *Applied Energy*. 2012;91:7-12.
- 35 [62] Li M, Zhang Y, Xu Y, Zhang D. Effect of different amounts of surfactant on characteristics of
36 nanoencapsulated phase-change materials. *Polym Bull*. 2011;67:541-52.
- 37 [63] Fuensanta M, Paiphansiri U, Romero-Sanchez MD, Guillem C, Lopez-Buendia AM, Landfester
38 K. Thermal properties of a novel nanoencapsulated phase change material for thermal energy
39 storage. *Thermochimica Acta*. 2013;565:95-101.
- 40 [64] Landfester K. Miniemulsions for Nanoparticle Synthesis. In: Antonietti M, editor. *Colloid*
41 *Chemistry II*: Springer Berlin Heidelberg; 2003. p. 75-123.
- 42
43
44
45
46
47
48
49
50
51
52
53
54
55
56
57
58
59
60
61
62
63
64
65

- 1 [65] Zhang XX, Tao XM, Yick KL, Wang XC. Structure and thermal stability of microencapsulated
2 phase-change materials. *Colloid and Polymer Science*. 2004;282:330-6.
- 3 [66] Fang Y, Kuang S, Gao X, Zhang Z. Preparation and characterization of novel
4 nanoencapsulated phase change materials. *Energy Conversion and Management*.
5 2008;49:3704-7.
- 6 [67] Thies C. Microencapsulation, in: *Kirk-Othmer Encyclopedia of Chemical Technology*. Wiley,
7 Hoboken, New Jersey: John Wiley & Sons Inc; 2006.
- 8 [68] Özonur Y, Mazman M, Paksoy HÖ, Evliya H. Microencapsulation of coco fatty acid mixture for
9 thermal energy storage with phase change material. *International Journal of Energy Research*.
10 2006;30:741-9.
- 11 [69] Onder E, Sarier N, Cimen E. Encapsulation of phase change materials by complex
12 coacervation to improve thermal performances of woven fabrics. *Thermochimica Acta*.
13 2008;467:63-72.
- 14 [70] Hawlader MNA, Uddin MS, Khin MM. Microencapsulated PCM thermal-energy storage
15 system. *Applied Energy*. 2003;74:195-202.
- 16 [71] Bayés-García L, Ventolà L, Cordobilla R, Benages R, Calvet T, Cuevas-Diarte MA. Phase
17 Change Materials (PCM) microcapsules with different shell compositions: Preparation,
18 characterization and thermal stability. *Solar Energy Materials and Solar Cells*. 2010;94:1235-40.
- 19 [72] Su JF, Huang Z, Ren L. High compact melamine-formaldehyde microPCMs containing
20 n-octadecane fabricated by a two-step coacervation method. *Colloid and Polymer Science*.
21 2007;285:1581-91.
- 22 [73] Zhang H, Wang X, Wu D. Silica encapsulation of n-octadecane via sol-gel process: A novel
23 microencapsulated phase-change material with enhanced thermal conductivity and performance.
24 *Journal of Colloid and Interface Science*. 2010;343:246-55.
- 25 [74] Wang L-Y, Tsai P-S, Yang Y-M. Preparation of silica microspheres encapsulating
26 phase-change material by sol-gel method in O/W emulsion. *Journal of Microencapsulation*.
27 2006;23:3-14.
- 28 [75] Li M, Wu Z, Tan J. Properties of form-stable paraffin/silicon dioxide/expanded graphite
29 phase change composites prepared by sol-gel method. *Applied Energy*. 2012;92:456-61.
- 30 [76] Fang G, Chen Z, Li H. Synthesis and properties of microencapsulated paraffin composites
31 with SiO₂ shell as thermal energy storage materials. *Chemical Engineering Journal*.
32 2010;163:154-9.
- 33 [77] Chang CC, Tsai YL, Chiu JJ, Chen H. Preparation of phase change materials microcapsules by
34 using PMMA network-silica hybrid shell via sol-gel process. *Journal of Applied Polymer Science*.
35 2009;112:1850-7.
- 36 [78] Chen Z, Cao L, Shan F, Fang G. Preparation and characteristics of microencapsulated stearic
37 acid as composite thermal energy storage material in buildings. *Energy and Buildings*.
38 2013;62:469-74.
- 39 [79] Chen Z, Cao L, Fang G, Shan F. Synthesis and Characterization of Microencapsulated Paraffin
40 Microcapsules as Shape-Stabilized Thermal Energy Storage Materials. *Nanoscale and Microscale
41 Thermophysical Engineering*. 2013;17:112-23.
- 42
43
44
45
46
47
48
49
50
51
52
53
54
55
56
57
58
59
60
61
62
63
64
65

- 1 [80] Sara TL, Mohammad M, Mehdi M, Meurah IMT, Simon CMH. Synthesis, characterization and
2 thermal properties of nanoencapsulated phase change materials via sol-gel method. *Energy*.
3 2013.
- 4 [81] Salaün F, Devaux E, Bourbigot S, Rumeau P. Influence of the solvent on the
5 microencapsulation of an hydrated salt. *Carbohydrate Polymers*. 2010;79:964-74.
- 6 [82] Wang TY, Huang J. Synthesis and characterization of microencapsulated sodium phosphate
7 dodecahydrate. *Journal of Applied Polymer Science*. 2013:n/a-n/a.
- 8 [83] Wang T, Huang J, Zhu P, Xiao J. Fabrication and characterization of micro-encapsulated
9 sodium phosphate dodecahydrate with different crosslinked polymer shells. *Colloid and Polymer
10 Science*. 2013:1-6.
- 11 [84] Huang J, Wang T, Zhu P, Xiao J. Preparation, characterization, and thermal properties of the
12 microencapsulation of a hydrated salt as phase change energy storage materials. *Thermochimica
13 Acta*. 2013.
- 14 [85] Loxley A, Vincent B. Preparation of Poly(methylmethacrylate) Microcapsules with Liquid
15 Cores. *Journal of Colloid and Interface Science*. 1998;208:49-62.
- 16 [86] Yang R, Zhang Y, Wang X, Zhang Y, Zhang Q. Preparation of n-tetradecane-containing
17 microcapsules with different shell materials by phase separation method. *Solar Energy Materials
18 and Solar Cells*. 2009;93:1817-22.
- 19 [87] Jiang Y, Wang D, Zhao T. Preparation, characterization, and prominent thermal stability of
20 phase-change microcapsules with phenolic resin shell and n-hexadecane core. *Journal of Applied
21 Polymer Science*. 2007;104:2799-806.
- 22 [88] Zhang Y, Lin W, Yang R, Zhang Q. Preparation and thermal property of phase change
23 material microcapsules by phase separation. 2007. p. 2293-6.
- 24 [89] Kim EY, Kim HD. Preparation and properties of microencapsulated octadecane with
25 waterborne polyurethane. *Journal of Applied Polymer Science*. 2005;96:1596-604.
- 26 [90] Yu S, Wang X, Wu D. Microencapsulation of n-octadecane phase change material with
27 calcium carbonate shell for enhancement of thermal conductivity and serving durability:
28 Synthesis, microstructure, and performance evaluation. *Applied Energy*. 2014;114:632-43.
- 29 [91] WATSON ES, WATSON ES. DIFFERENTIAL MICROCALORIMETER. U.S.1962.
- 30 [92] Darkwa J, Su O, Zhou T. Development of non-deform micro-encapsulated phase change
31 energy storage tablets. *Applied Energy*. 2012;98:441-7.
- 32 [93] Sarl A. Form-stable paraffin/high density polyethylene composites as solid-liquid phase
33 change material for thermal energy storage: preparation and thermal properties. *Energy
34 Conversion and Management*. 2004;45:2033-42.
- 35 [94] Wang H-Y, Lu S-S. Study on thermal properties of phase change material by an optical DSC
36 system. *Applied Thermal Engineering*. 2013.
- 37 [95] Zhang Y, Yi J, Yi J. A simple method, the T-history method, of determining the heat of fusion,
38 specific heat and thermal conductivity of phase-change materials. *Meas Sci Technol*.
39 1999;10:201-5.
- 40 [96] Günther E, Hiebler S, Mehling H, Redlich R. Enthalpy of phase change material as function of
41 temperature - required accuracy and suitable measurement methods. *Int J Thermophys*.
42 2009;30:1257-69.
- 43
44
45
46
47
48
49
50
51
52
53
54
55
56
57
58
59
60
61
62
63
64
65

- 1 [97] Desgrosseilliers L, Allred P, Groulx D, White MA. Determination of
2 Enthalpy-Temperature-Composition Relations in Incongruent-Melting Phase Change Materials.
3 Applied Thermal Engineering. 2013.
- 4 [98] Meng D, Wang L. Characterization and thermal conductivity of modified graphite/fatty acid
5 eutectic/PMMA form-stable phase change material. J Wuhan Univ Technol-Mat Sci Edit.
6 2013;28:586-91.
- 7 [99] Wang J, Xie H, Xin Z, Li Y, Chen L. Enhancing thermal conductivity of palmitic acid based
8 phase change materials with carbon nanotubes as fillers. Solar Energy. 2010;84:339-44.
- 9 [100] Hunger M, Entrop AG, Mandilaras I, Brouwers HJH, Founti M. The behavior of
10 self-compacting concrete containing micro-encapsulated Phase Change Materials. Cement and
11 Concrete Composites. 2009;31:731-43.
- 12 [101] Zhao G, Xu X, Qiu L, Zheng X, Tang D. Study on the heat conduction of phase-change
13 material microcapsules. J Therm Sci. 2013;22:257-60.
- 14 [102] Cahill DG. Thermal conductivity measurement from 30 to 750 K: the 3 omega method.
15 Review of Scientific Instruments. 1990;61:802-8.
- 16 [103] Darkwa K, Kim JS. Dynamics of energy storage in phase change drywall systems.
17 International Journal of Energy Research. 2005;29:335-43.
- 18 [104] Marchi S, Pagliolico S, Sassi G. Characterization of panels containing micro-encapsulated
19 Phase Change Materials. Energy Conversion and Management. 2013;74:261-8.
- 20 [105] Sharma A, Sharma SD, Buddhi D. Accelerated thermal cycle test of acetamide, stearic acid
21 and paraffin wax for solar thermal latent heat storage applications. Energy Conversion and
22 Management. 2002;43:1923-30.
- 23 [106] Zhang Z, Saunders R, Thomas CR. Mechanical strength of single microcapsules determined
24 by a novel micromanipulation technique. J Microencapsul. 1999;16:117-24.
- 25 [107] Sun G, Zhang Z. Mechanical properties of melamine-formaldehyde microcapsules. J
26 Microencapsul. 2001;18:593-602.
- 27 [108] Sun G, Zhang Z. Mechanical strength of microcapsules made of different wall materials.
28 International Journal of Pharmaceutics. 2002;242:307-11.
- 29 [109] Hu J, Chen H-Q, Zhang Z. Mechanical properties of melamine formaldehyde microcapsules
30 for self-healing materials. Materials Chemistry and Physics. 2009;118:63-70.
- 31 [110] Su J, Ren L, Wang L. Preparation and mechanical properties of thermal energy storage
32 microcapsules. Colloid and Polymer Science. 2005;284:224-8.
- 33
34
35
36
37
38
39
40
41
42
43
44
45
46
47
48
49
50
51
52
53
54
55
56
57
58
59
60
61
62
63
64
65

Figure 1

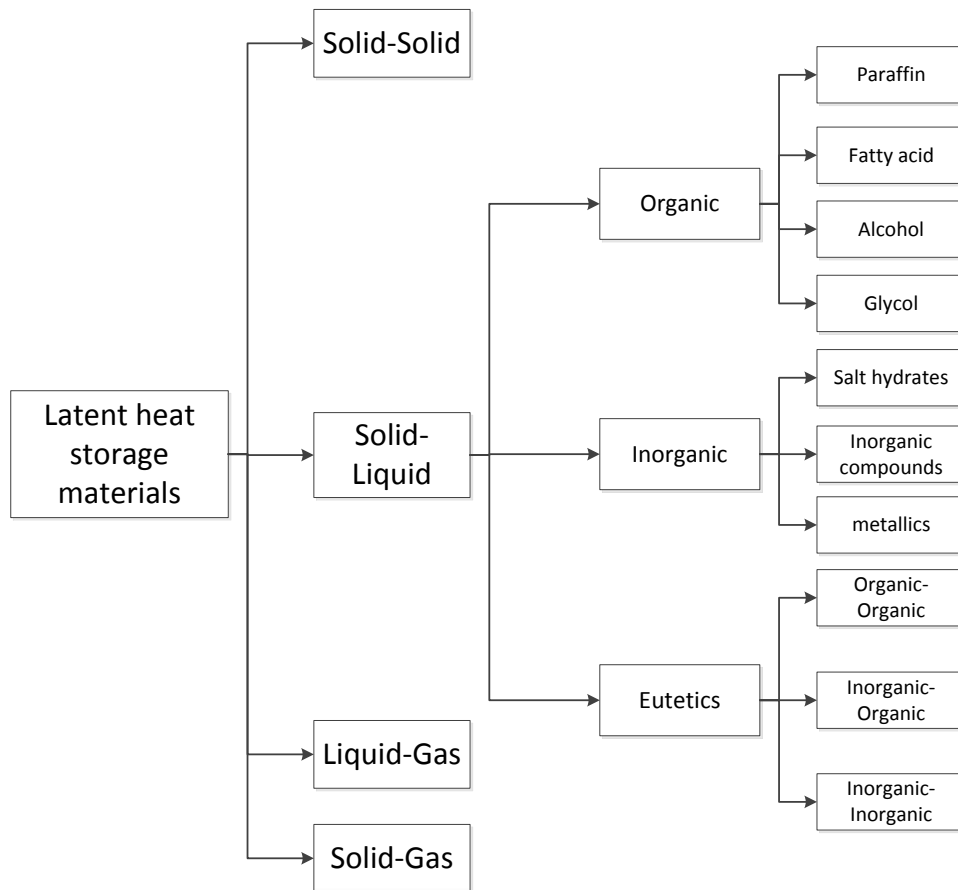


Figure 1 Classification of PCMs

Figure 2

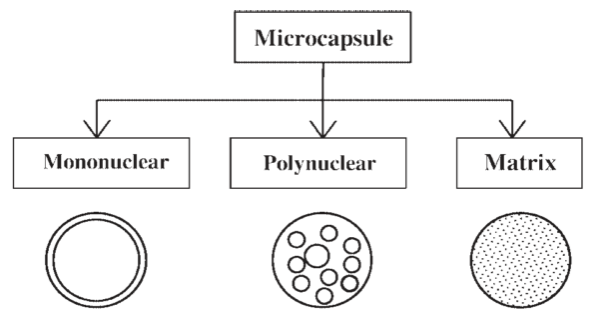


Figure 2 Structure of MEPCMs/NEPCMs

Figure 3

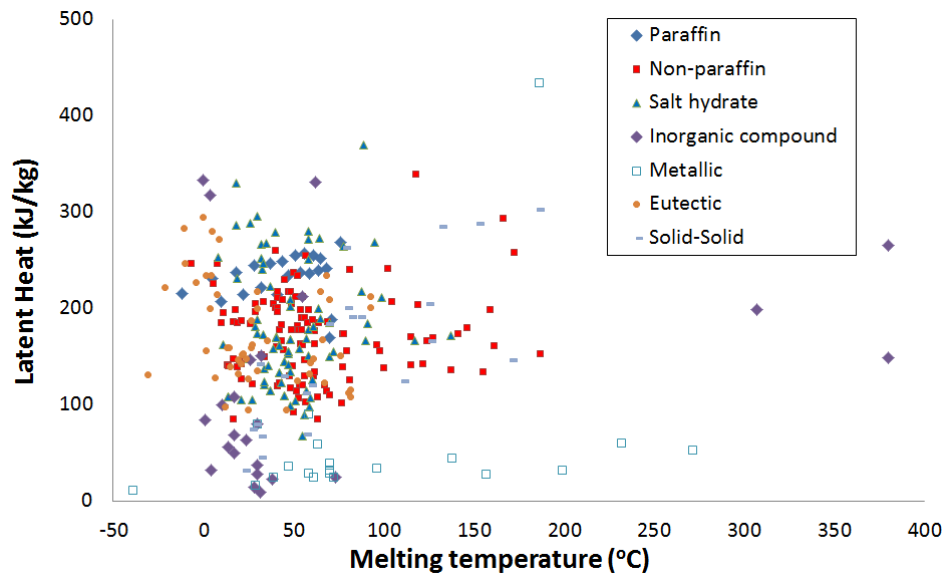


Figure 3 Melting temperature and latent heat distribution for different types of PCMs

Figure 4

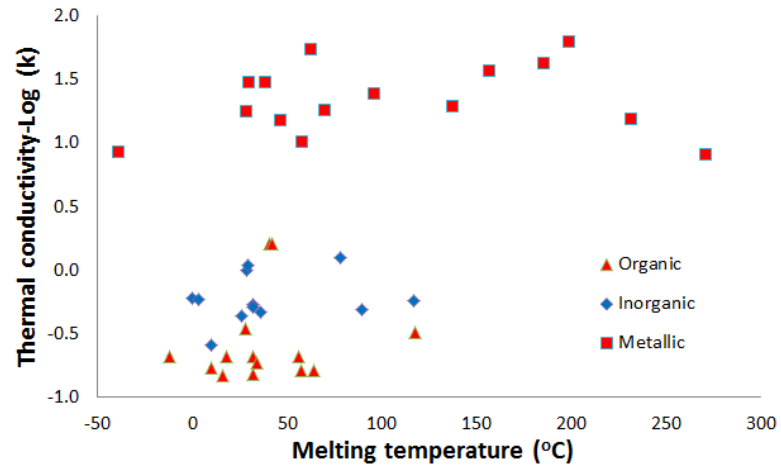


Figure 4 Thermal conductivity distribution for different types of PCMs

Figure 5

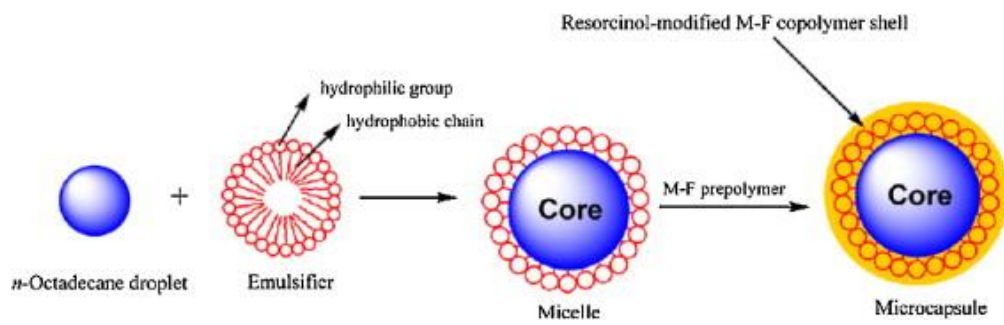


Figure 5 Fabrication of the MEPCM by in-situ polymerization

Figure 6

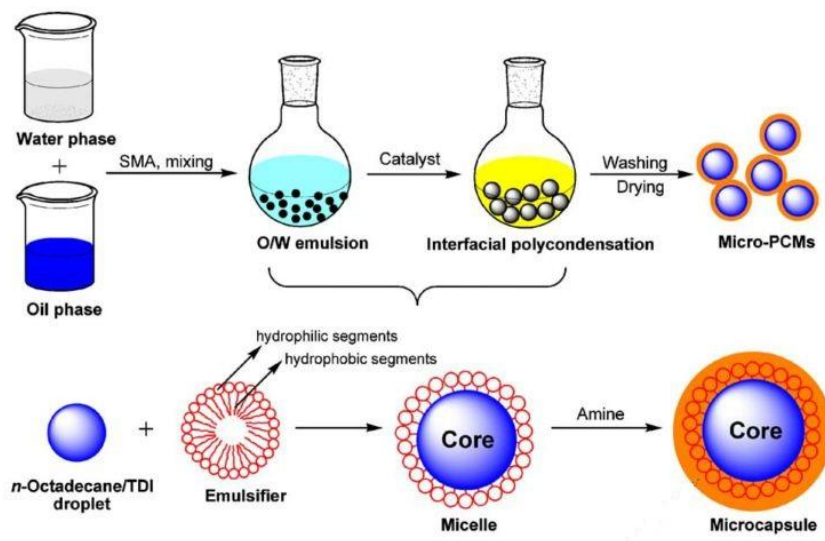


Figure 6 Microcapsule manufactured by interfacial polycondensation

Figure 7

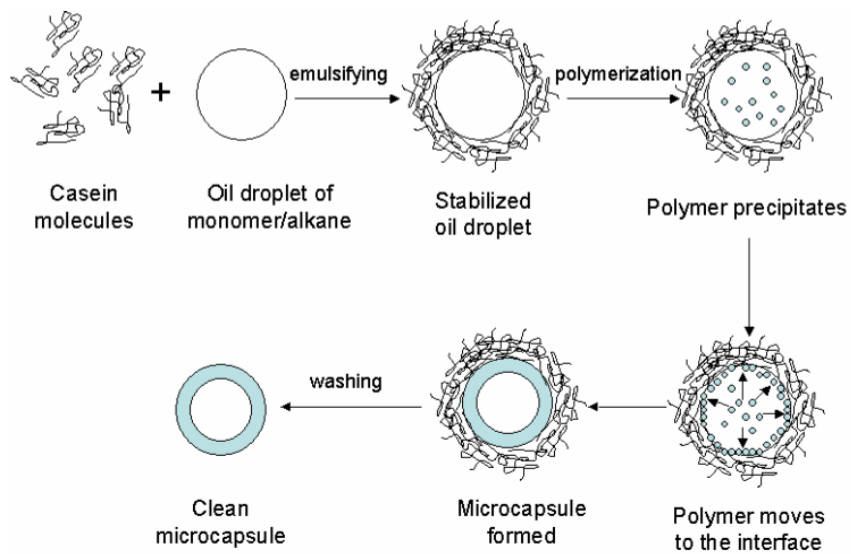


Figure 7 Schematic of the fabrication MEPCM by suspension-like polymerization

Figure 8

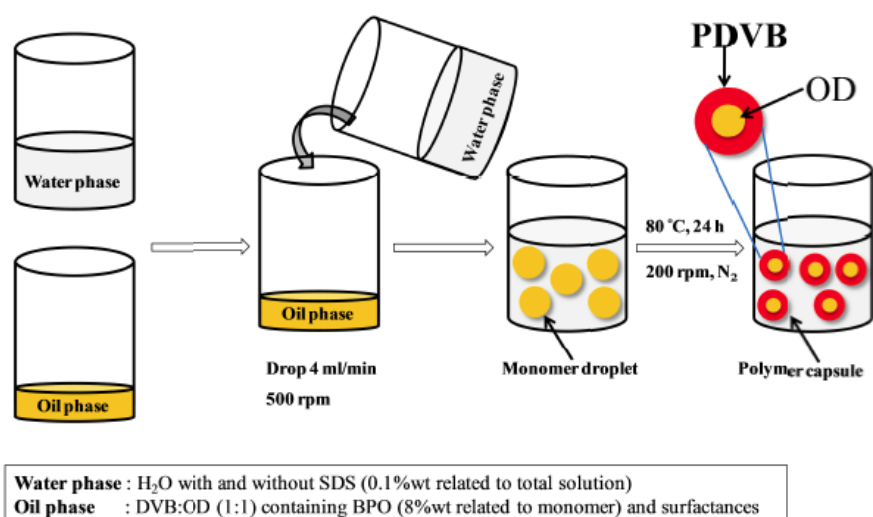


Figure 8 Schematic of the preparation of the PDVB/Octadecane capsules by the microsuspension polymerization

Figure 9

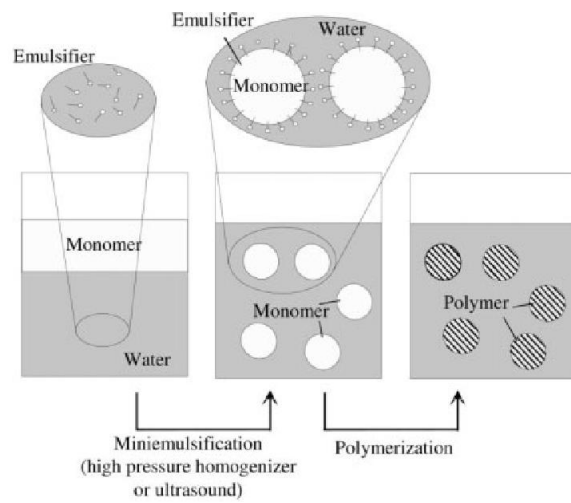


Figure 9 The procedure of miniemulsion polymerization

Figure 10

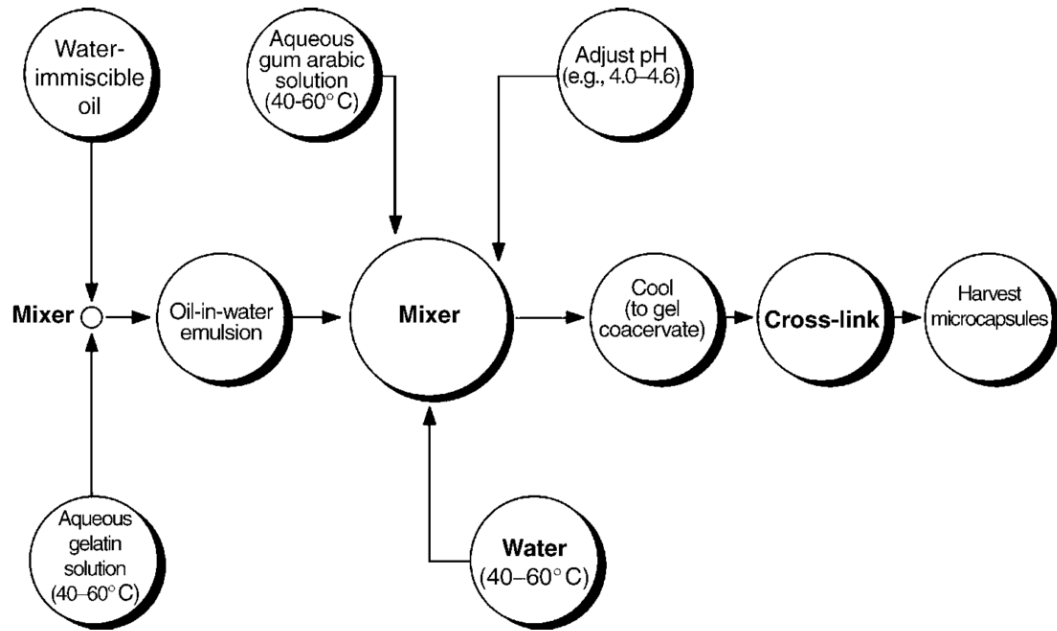


Figure 10 Flow diagram of a typical encapsulation process based on the complex coacervation

Figure 11

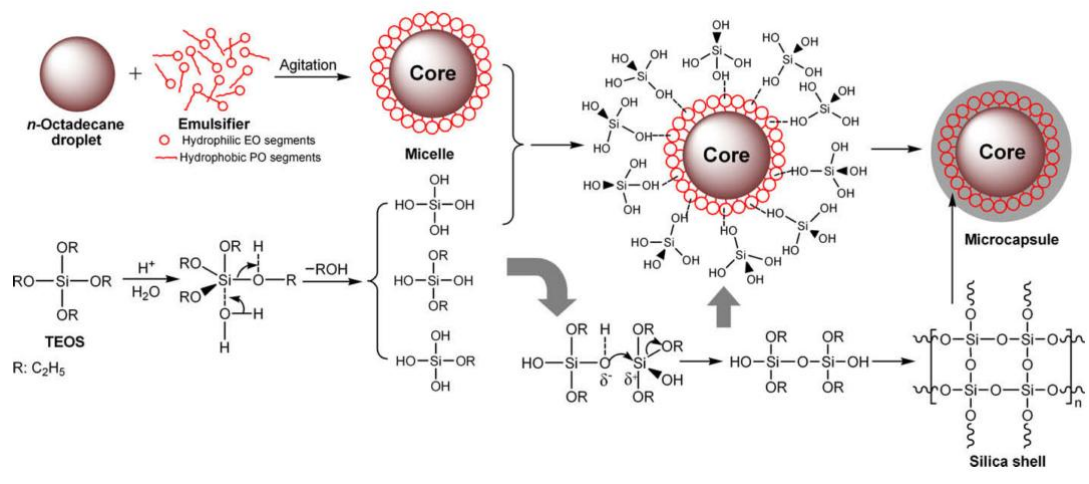


Figure 11 Schematic formation of a sol-gel process

Figure 12

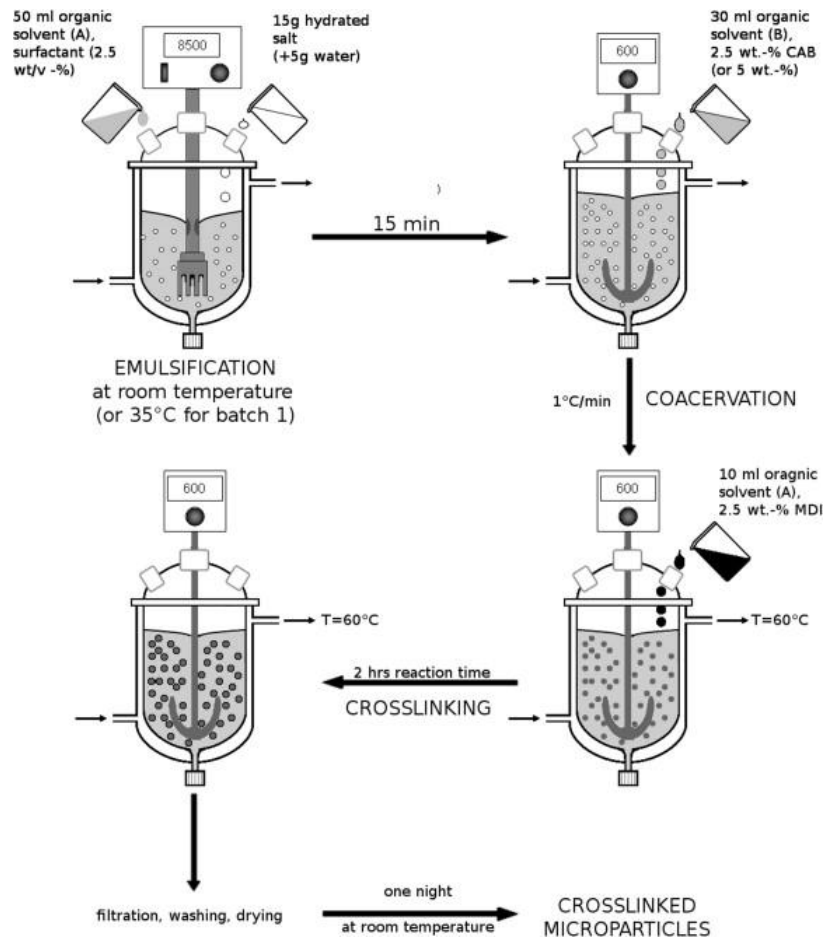


Figure 12 Schematic overview of microencapsulation by solvent extraction/evaporation method

Figure 13

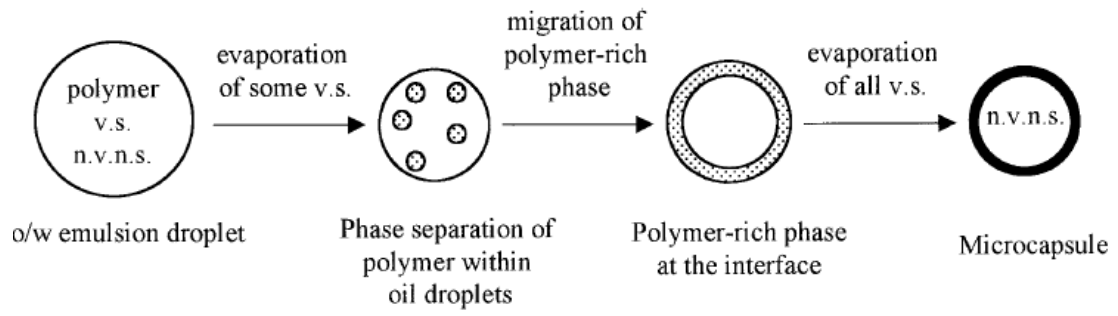


Figure 13 Schematic of the encapsulation process

Figure 15

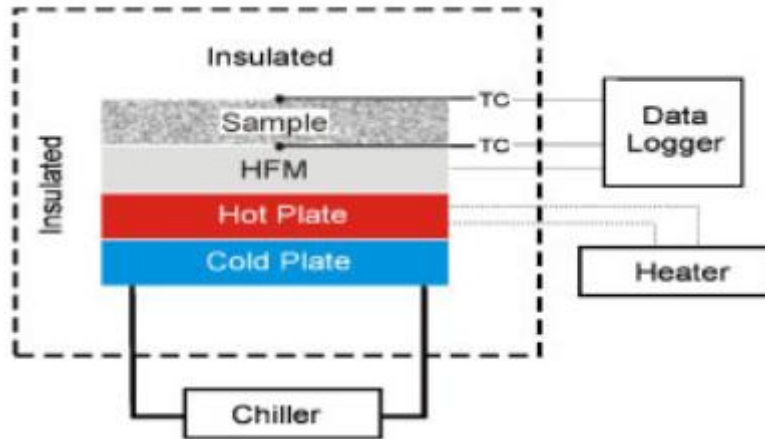


Figure 15 Thermal conductivity testing rig

Figure 16

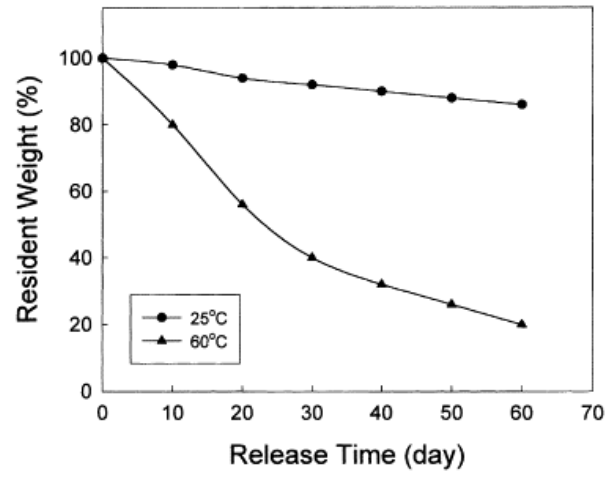


Figure 16 Resident weight (%) of melamine resin microcapsules in long self-life test

Figure 17

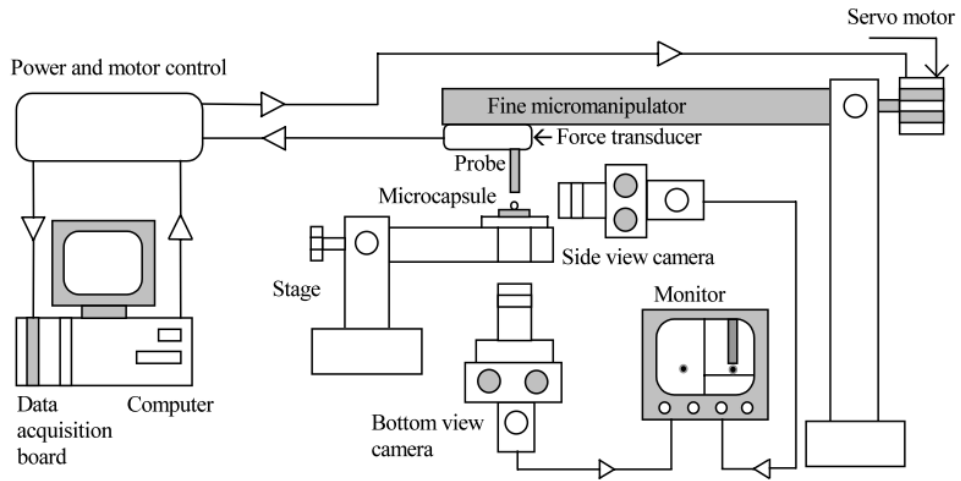


Figure 17 Schematic diagram of the micromanipulation rig

Figure 18

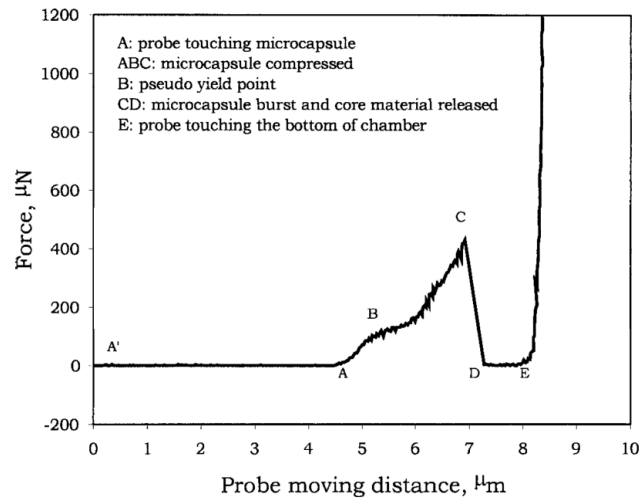


Figure 18 Force versus probe moving distance

Table 1: Thermophysical properties of paraffin

Name	T _m (°C)	H (kJ/kg)	k (W/m·K)	ρ(kg/m ³)	C _p (kJ/kg)
n -Dodecane	-12	216	0.21(s),0.21(l)	750	n.a.
n -Tridecane	-6	n.a.	n.a.	756	n.a.
n -Tetradecane	4.5-5.6	231	n.a.	771	n.a.
n -Pentadecane	10	207	0.17	768	n.a.
n -Hexadecane	18.2	238	0.21(s)	774	n.a.
n -Heptadecane	22	215	n.a.	778	n.a.
n -Octadecane	28.2	245	0.35(s),0.149(l)	814(s),775(l)	2.14(s),2.66(l)
n -Nonadecane	31.9	222	0.21(s)	912(s),769(l)	n.a.
n -Eicosane	37	247	n.a.	n.a.	n.a.
n -Heneicosane	41	215	n.a.	n.a.	n.a.
n -Docosane	44	249	n.a.	n.a.	n.a.
n -Tricosane	47	234	n.a.	n.a.	n.a.
n -Tetracosane	51	255	n.a.	n.a.	n.a.
n -Pentacosane	54	238	n.a.	n.a.	n.a.
n -Hexacosane	56	257	0.21(s)	770	n.a.
n -Heptacosane	59	236	n.a.	773	n.a.
n -Octacosane	61	255	n.a.	910(s),765(l)	n.a.
n -Nonacosane	64	240	n.a.	n.a.	n.a.
n -Triacontane	65	252	n.a.	n.a.	n.a.
n -Hentriacontane	68	242	n.a.	930(s),830(l)	n.a.
n -Dotriacontane	70	170	n.a.	n.a.	n.a.
n -Tritriacontane	71	189	n.a.	n.a.	n.a.
n -Tetratriacontane	75.9	269	n.a.	772.8(s)	n.a.

Legend:

C_p: Specific heat (kJ/kg)

H: Latent heat (kJ/kg)

k: Thermal conductivity (W/m·K)

T_m: Melting temperature (°C)

ρ: Density (kg/m³)

Table 2: Thermophysical properties of non-paraffin PCMs

Name	T_m (°C)	H (kJ/kg)	k (W/m·K)	ρ (kg/m ³)	Cp (kJ/kg)
Triethylene glycol	-7	247	n.a.	1200(l)	n.a.
N-Tetradecane	5.5	226	n.a.	n.a.	n.a.
Formic acid	7.8	247	n.a.	1226.7	n.a.
Dimethyl adipate[13]	9.7	164.6	0.358	1062	n.a.
Propyl palmitate	10	186	n.a.	n.a.	n.a.
Tetrabutyl ammoniumbromide (type A-type B)	10–12	193–199	n.a.	n.a.	n.a.
Isopropyl palmitate	11	n.a.	n.a.	n.a.	n.a.
Oleic acid	13.5-16.3	n.a.	n.a.	863	n.a.
Isopropyl stearate	14-19	140-142	n.a.	n.a.	n.a.
Caprylic acid	16.3	148	0.149	901	n.a.
Dimethyl sulfoxide	16.5	85.7	n.a.	1009(l)	n.a.
Acetic acid	16.7	187-273	n.a.	1050	n.a.
Glycerin	17.9	198.7	n.a.	1260	n.a.
Butyl stearate	19	140	n.a.	n.a.	n.a.
Propyl palmitate	19	186	n.a.	n.a.	n.a.
Polyethylene glycol 600	20-25	146	n.a.	1100	n.a.
Lithium chloride ethanolate	21	188	n.a.	n.a.	n.a.
Dimethyl sabacate	21	120-135	n.a.	n.a.	n.a.
Octadecyl 3-mencaptopropylate	21	143	n.a.	n.a.	n.a.
D-Lactic acid	26	184	n.a.	1249	n.a.
Vinyl stearate	27-29	122	n.a.	n.a.	n.a.
Acid Methyl pentacosane	29	197	n.a.	n.a.	n.a.
Methyl palmitate	29	205	n.a.	n.a.	n.a.
Capric acid	32	152.7	0.153	878	n.a.
Erucic acid	33	n.a.	n.a.	853	n.a.
Trimyristin	33-57	201-213	n.a.	862	n.a.
Polyethelene glycol 900 (PEG900)	34	150.5	0.188	1100 (l) 1200 (s)	2.26
Camphenilone	39	205	n.a.	n.a.	n.a.
Caprilone	40	260	n.a.	n.a.	n.a.
Docasyl bromide	40	201	n.a.	n.a.	n.a.
n-Henicosane	40.5	161	n.a.	n.a.	n.a.
Phenol	41	120	n.a.	n.a.	n.a.
Heptadecanone	41	201	n.a.	n.a.	n.a.
1-Cyclohexyloctadecane	41	218	n.a.	n.a.	n.a.
4-Heptadacanone	41	197	n.a.	n.a.	n.a.
Stearic acid	41–43	211.6	1.6	862(l) 1007(s)	2.27(l)

					1.76(s)
Methyl-12-hydroxy-stearate	42–43	120–126	n.a.	n.a.	n.a.
Lauric acid	42–44	178	1.6	1007(s),862(l)	2.27(l) 1.76(s)
n-Lauric acid	43	183	n.a.	n.a.	n.a.
p-Joluidine	43.3	167	n.a.	n.a.	n.a.
Cyanamide	44	209	n.a.	1080	n.a.
N-Docosane	44.5	157	n.a.	n.a.	n.a.
Methyl eicosanate	45	230	n.a.	851	n.a.
Elaidic acid	47	218	n.a.	851	n.a.
n-Tricosane	47.6	130	n.a.	n.a.	n.a.
Pelargonic acid	48		n.a.	n.a.	n.a.
3-Heptadecanone	48	218	n.a.	n.a.	n.a.
2-Heptadecanone	48	218	n.a.	n.a.	n.a.
Hydrocinnamic acid	48	118	n.a.	n.a.	n.a.
Cetyl alcohol	49.3	141	n.a.	n.a.	n.a.
Camphene	50	238	n.a.	842	n.a.
a-Nephthylamine	50	93	n.a.	n.a.	n.a.
O-Nitroaniline	50	93	n.a.	n.a.	n.a.
9-Heptadecanone	51	213	n.a.	n.a.	n.a.
Thymol	51.5	115	n.a.	n.a.	n.a.
Methyl behenate	52	234	n.a.	n.a.	n.a.
Myristic acid	52.2-58	182.6-199	n.a.	862.2	n.a.
Pentadecanoic acid	52.5	178	n.a.	n.a.	n.a.
Diphenyl amine	52.9	107	n.a.	n.a.	n.a.
P-Dichlorobenzene	53.1	121	n.a.	n.a.	n.a.
N-Pentacosane	53.7	164	n.a.	n.a.	n.a.
Oxolate	54.3	178	n.a.	n.a.	n.a.
Tristearin	54.5	191	n.a.	n.a.	n.a.
Hypophosphoric acid	55	213	n.a.	n.a.	n.a.
O-Xylene dichloride	55	121	n.a.	n.a.	n.a.
Palmatic acid	55	163	n.a.	n.a.	n.a.
β Chloroacetic acid	56	147	n.a.	n.a.	n.a.
Chloroacetic acid	56	130	n.a.	1580	n.a.
N-Hexacosane	56.3	255	n.a.	n.a.	n.a.
Nitro naphthalene	56.7	103	n.a.	n.a.	n.a.
Palmitic acid	57.8–61.8	185.4	0.162	850 (l) 989 (s)	n.a.
Heptaudecanoic acid	60.6	189	n.a.	n.a.	n.a.
α-Chloroacetic acid	61.2	130	n.a.	n.a.	n.a.
n-Octacosane	61.4	134	n.a.	n.a.	n.a.
Bee wax	61.8	177	n.a.	950	n.a.
Glycolic acid	63	109	n.a.	n.a.	n.a.
P-Bromophenol	63.5	86	n.a.	n.a.	n.a.
Azobenzene	67.1	121	n.a.	n.a.	n.a.

Acrylic acid	68	115	n.a.	n.a.	n.a.
Dintro toluene (2,4)	70	111	n.a.	n.a.	n.a.
Oxazoline wax-TS 970	74	n.a.	n.a.	n.a.	n.a.
Arachic acid	76.5	n.a.	n.a.	n.a.	n.a.
Phenylacetic acid	76.7	102	n.a.	n.a.	n.a.
Thiosinamine	77	140	n.a.	n.a.	n.a.
Bromcamphor	77	174	n.a.	1449	n.a.
Benzylamine	78	174	n.a.	n.a.	n.a.
Durene	79.3	156	n.a.	838	n.a.
Acetamide	81	241	n.a.	1159	n.a.
Methyl brombrenzoate	81	126	n.a.	n.a.	n.a.
Alpha naphthol	96	163	n.a.	1095	n.a.
Glutaric acid	97.5	156	n.a.	1429	n.a.
p-Xylene dichloride	100	138.7	n.a.	n.a.	n.a.
Methyl fumarate	102	242	n.a.	1045	n.a.
Catechol	104.3	207	n.a.	1370	n.a.
Quinone	115	171	n.a.	1318	n.a.
Acetanilide	115	142	n.a.	1210	n.a.
Erythritol	117.7	339.8	0.326(l) 0.733(s)	1300 (l) 1480 (s)	2.61(l) 2.25(s)
Succinic anhydride	119	204	n.a.	1104	n.a.
Valporic acid	120	n.a.	n.a.	n.a.	n.a.
Benzoic acid	121.7	142.8	n.a.	1266	n.a.
Stibene	124	167	n.a.	1164	n.a.
Benzamide	127.2	169.4	n.a.	1341	n.a.
Phenacetin	137	136.7	n.a.	n.a.	n.a.
Acetyl-p-toluidene	146	180	n.a.	n.a.	n.a.
Phenylhdrazone	155	134.8	n.a.	n.a.	n.a.
Benzaldehyde	159	199	n.a.	1443	n.a.
Benzanilide	161	162	n.a.	n.a.	n.a.
O-Mannitol	166	294	n.a.	1489	n.a.
Hydroquinone	172.4	258	n.a.	1358	n.a.
p-Aminobenzoic acid	187	153	n.a.	n.a.	n.a.

Table 3: Thermophysical properties of salt hydrates

Name	Chemical Formula	T _m (°C)	H (kJ/kg)	k (W/m·K)	ρ (kg/m ³)	C _p (kJ/kg)
Lithium chlorate trihydrate	LiClO ₃ ·3H ₂ O	8	253	n.a.	1720(s), 1530(l)	n.a.
Zinc chloride trihydrate	ZnCl ₂ ·3H ₂ O	10	n.a.	n.a.	n.a.	n.a.
Ammonium chloride Sodium sulfate decahydrate	NH ₄ Cl·Na ₂ SO ₄ ·10H ₂ O	11	163	n.a.	n.a.	n.a.
Dipotassium hydrogen phosphate hexahydrate	K ₂ HPO ₄ ·6H ₂ O	14	109	n.a.	n.a.	n.a.
Sodium chloride Sodium sulfate decahydrate	NaCl·Na ₂ SO ₄ ·10H ₂ O	18	286	n.a.	n.a.	n.a.
Potassium fluoride tetrahydrate	KF·4H ₂ O	18	330	n.a.	n.a.	n.a.
Dipotassium hydrogen phosphate tetrahydrate	K ₂ HPO ₄ ·4H ₂ O	18.5	231	n.a.	1447(l), 1480(s)	1.84(s), 2.39(l)
Iron bromide hexahydrate	FeBr ₃ ·6H ₂ O	21	105	n.a.	n.a.	n.a.
Manganese nitrate hexahydrate	Mn(NO ₃) ₂ ·6H ₂ O	25.5	125.9- 148	n.a.	1738(s), 1728(l)	n.a.
Lithium metaborate octahydrate	LiBO ₂ ·8H ₂ O	25.7	289	n.a.	n.a.	n.a.
Calcium chloride hexahydrate	CaCl ₂ ·6H ₂ O	29–3 0	170–1 92	1.008(s),0 .561(l)	1802(s), 1562(l)	n.a.
Calcium chloride dodecahydrate	CaCl ₂ ·12H ₂ O	29.8	174	1.09(s),0. 53(l)	1710(s), 1530(s)	1.4(s), 2.2(l)
Lithium nitrate trihydrate	LiNO ₃ ·3H ₂ O	30	189–2 96	n.a.	n.a.	n.a.
Lithium nitrate dihydrate	LiNO ₃ ·2H ₂ O	30	296	n.a.	n.a.	n.a.
Sodium sulfate decahydrate	Na ₂ SO ₄ ·10H ₂ O	32	251–2 54	0.544	1485(s)	2
Sodium carbonate decahydrate	Na ₂ CO ₃ ·10H ₂ O	32	267	0.514(s), 0.224(l)	830	1.92(s), 3.26(l)
Iron potassium alum	KFe(SO ₄) ₂ ·12H ₂ O	33	173	n.a.	n.a.	n.a.
Calcium bromide hexahydrate	CaBr ₂ ·6H ₂ O	34	115–1 38	n.a.	2194(s), 1956(l)	n.a.
Lithium bromide dihydrate	LiBr·2H ₂ O	34	124	n.a.	n.a.	n.a.
Dipotassium hydrogen phosphate dodecahydrate	Na ₂ HPO ₄ ·12H ₂ O	35–4 0	256–2 81	n.a.	1522	n.a.

Zinc hexahydrate	nitrate	$\text{Zn}(\text{NO}_3)_2 \cdot 6\text{H}_2\text{O}$	36	134–1 47	0.464	1937(s), 1828(l)	n.a.
Manganese tetrahydrate	nitrate	$\text{Mn}(\text{NO}_3)_2 \cdot 4\text{H}_2\text{O}$	37	115	n.a.	n.a.	n.a.
Iron hexahydrate	chloride	$\text{FeCl}_3 \cdot 6\text{H}_2\text{O}$	37	223	n.a.	n.a.	n.a.
Calcium tetrahydrate	chloride	$\text{CaCl}_2 \cdot 4\text{H}_2\text{O}$	39	158	n.a.	n.a.	n.a.
Copper heptahydrate	Sulfate	$\text{CuSO}_4 \cdot 7\text{H}_2\text{O}$	40.7	171	n.a.	n.a.	n.a.
Potassium dihydrate	fluoride	$\text{KF} \cdot 2\text{H}_2\text{O}$	42	162–2 66	n.a.	n.a.	n.a.
Magnesium octahydrate	iodide	$\text{MgI}_2 \cdot 8\text{H}_2\text{O}$	42	133	n.a.	n.a.	n.a.
Calcium hexahydrate	iodide	$\text{CaI}_2 \cdot 6\text{H}_2\text{O}$	42	162	n.a.	n.a.	n.a.
Calcium tetrahydrate	nitrate	$\text{Ca}(\text{NO}_3)_2 \cdot 4\text{H}_2\text{O}$	43–4 7	106–1 40	n.a.	n.a.	n.a.
Zinc tetrahydrate	nitrate	$\text{Zn}(\text{NO}_3)_2 \cdot 4\text{H}_2\text{O}$	45	110	n.a.	n.a.	n.a.
Tripotassium phosphate tribasic heptahydrate		$\text{K}_3\text{PO}_4 \cdot 7\text{H}_2\text{O}$	45	145	n.a.	n.a.	n.a.
Dipotassium phosphate heptahydrate	hydrogen	$\text{K}_2\text{HPO}_4 \cdot 7\text{H}_2\text{O}$	45	145	n.a.	n.a.	n.a.
Iron nonahydrate	nitrate	$\text{Fe}(\text{NO}_3)_3 \cdot 9\text{H}_2\text{O}$	47	155–1 90	n.a.	n.a.	n.a.
Magnesium tetrahydrate	nitrate	$\text{Mg}(\text{NO}_3)_2 \cdot 4\text{H}_2\text{O}$	47	142	n.a.	n.a.	n.a.
Sodium pentahydrate	sulfite	$\text{Na}_2\text{SiO}_3 \cdot 5\text{H}_2\text{O}$	48	168	n.a.	n.a.	n.a.
Sodium tetrahydrate	sulfit	$\text{Na}_2\text{SiO}_3 \cdot 4\text{H}_2\text{O}$	48	168	n.a.	n.a.	n.a.
Dipotassium phosphate heptahydrate	hydrogen	$\text{Na}_2\text{HPO}_4 \cdot 7\text{H}_2\text{O}$	48	135–1 70	n.a.	n.a.	n.a.
Sodium pentahydrate	thiosulfate	$\text{Na}_2\text{S}_2\text{O}_3 \cdot 5\text{H}_2\text{O}$	48	209	n.a.	1600	n.a.
Dipotassium phosphate trihydrate	hydrogen	$\text{K}_2\text{HPO}_4 \cdot 3\text{H}_2\text{O}$	48	99	n.a.	n.a.	n.a.
Magnesium heptahydrate	sulfate	$\text{MgSO}_4 \cdot 7\text{H}_2\text{O}$	48.5	202	n.a.	n.a.	n.a.
Calcium trihydrate	nitrate	$\text{Ca}(\text{NO}_3)_2 \cdot 3\text{H}_2\text{O}$	51	104	n.a.	n.a.	n.a.

Sodium hexahydrate	nitrate	$\text{Na}(\text{NO}_3)_2 \cdot 6\text{H}_2\text{O}$	53	158	n.a.	n.a.	n.a.
Zinc nitrate dihydrate		$\text{Zn}(\text{NO}_3)_2 \cdot 2\text{H}_2\text{O}$	55	68	n.a.	n.a.	n.a.
Iron chloride dihydrate		$\text{FeCl}_3 \cdot 2\text{H}_2\text{O}$	56	90	n.a.	n.a.	n.a.
Cobaltous hexahydrate	nitrate	$\text{Co}(\text{NO}_3)_2 \cdot 6\text{H}_2\text{O}$	57	115	n.a.	n.a.	n.a.
Nick hexahydrate	nitrate	$\text{Ni}(\text{NO}_3)_2 \cdot 6\text{H}_2\text{O}$	57	169	n.a.	n.a.	n.a.
Manganese tetrahydrate	chloride	$\text{MnCl}_2 \cdot 4\text{H}_2\text{O}$	58	151	n.a.	n.a.	n.a.
Sodium trihydrate	acetate	$\text{CH}_3\text{COONa} \cdot 3\text{H}_2\text{O}$	58	270–290	n.a.	1450	n.a.
Lithium dihydrate	acetate	$\text{LiC}_2\text{H}_3\text{O}_2 \cdot 2\text{H}_2\text{O}$	58	251–377	n.a.	n.a.	n.a.
Magnesium tetrahydrate	chloride	$\text{MgCl}_2 \cdot 4\text{H}_2\text{O}$	58	178	n.a.	n.a.	n.a.
Sodium monohydrate	hydroxide	$\text{NaOH} \cdot \text{H}_2\text{O}$	58	272	n.a.	n.a.	n.a.
Cadmium tetrahydrate	nitrate	$\text{Cd}(\text{NO}_3)_2 \cdot 4\text{H}_2\text{O}$	59	98	n.a.	n.a.	n.a.
Cadmium monohydrate	nitrate	$\text{Cd}(\text{NO}_3)_2 \cdot 1\text{H}_2\text{O}$	59.5	107	n.a.	n.a.	n.a.
Iron hexahydrate	nitrate	$\text{Fe}(\text{NO}_3)_2 \cdot 6\text{H}_2\text{O}$	60.5	126	n.a.	n.a.	n.a.
Sodium sulfate dodecahydrate	aluminum	$\text{NaAl}(\text{SO}_4)_2 \cdot 12\text{H}_2\text{O}$	61	181	n.a.	n.a.	n.a.
Sodium sulfate decahydrate	aluminum	$\text{NaAl}(\text{SO}_4)_2 \cdot 10\text{H}_2\text{O}$	61	181	n.a.	n.a.	n.a.
Ferrous Heptahydrate	Sulfate	$\text{FeSO}_4 \cdot 7\text{H}_2\text{O}$	64	200	n.a.	n.a.	n.a.
Sodium dodecahydrate	phosphate	$\text{Na}_3\text{PO}_4 \cdot 12\text{H}_2\text{O}$	65	190	n.a.	n.a.	n.a.
Sodium decahydrate	borate	$\text{Na}_2\text{B}_4\text{O}_7 \cdot 10\text{H}_2\text{O}$	68	n.a.	n.a.	n.a.	n.a.
Lithium dihydrate	ethanoate	$\text{LiCH}_3\text{COO} \cdot 2\text{H}_2\text{O}$	70	150–251	n.a.	n.a.	n.a.
Sodium decahydrate	polyphosphate	$\text{Na}_2\text{P}_2\text{O}_7 \cdot 10\text{H}_2\text{O}$	70	186–230	n.a.	n.a.	n.a.
Aluminium nonahydrate	nitrate	$\text{Al}(\text{NO}_3)_3 \cdot 9\text{H}_2\text{O}$	72	155–176	n.a.	n.a.	n.a.
Barium octahydrate	hydroxide	$\text{Ba}(\text{OH})_2 \cdot 8\text{H}_2\text{O}$	78	265–280	1.255(s),0.653(l)	2070(s),1937(l)	n.a.
Aluminium 18-hydrate	sulfate	$\text{Al}_2(\text{SO}_4)_3 \cdot 18\text{H}_2\text{O}$	88	218	n.a.	n.a.	n.a.

Strontium hydroxide octahydrate	$\text{Sr}(\text{OH})_2 \cdot 8\text{H}_2\text{O}$	89	370	n.a.	n.a.	n.a.
Magnesium nitrate hexahydrate	$\text{Mg}(\text{NO}_3)_2 \cdot 6\text{H}_2\text{O}$	89.9	167	0.490(l), .611(s)	1550(l), 1636(s)	n.a.
Aluminum potassium sulfate dodecahydrate	$\text{KAl}(\text{SO}_4)_2 \cdot 12\text{H}_2\text{O}$	91	184	n.a.	n.a.	n.a.
Ammonium alum	$(\text{NH}_4)\text{Al}(\text{SO}_4)_2 \cdot 6\text{H}_2\text{O}$	95	269	n.a.	n.a.	n.a.
Lithium chloride monohydrate	$\text{LiCl} \cdot \text{H}_2\text{O}$	99	212	n.a.	n.a.	n.a.
Calcium bromide tetrahydrate	$\text{CaBr}_2 \cdot 4\text{H}_2\text{O}$	110	n.a.	n.a.	n.a.	n.a.
Aluminium sulfate 16-hydrate	$\text{Al}_2(\text{SO}_4)_3 \cdot 16\text{H}_2\text{O}$	112	n.a.	n.a.	n.a.	n.a.
Magnesium chloride hexahydrate	$\text{MgCl}_2 \cdot 6\text{H}_2\text{O}$	117	167	0.570(l), 0.704(s)	1450(l), 1570(s)	2.61(l), 2.25(s)

Table 4: Thermal physical properties of inorganic compounds

Name	Chemical Formula	T _m (°C)	H (kJ/kg)	k (W/m·K)
Water	H ₂ O	0	333	0.598
Phosphorus oxychloride	POCl ₃	1	85	n.a.
Deuterium oxide	D ₂ O	3.7	318	0.595
Antimony chloride	SbCl ₅	4	33	n.a.
Sulfuric acid	H ₂ SO ₄	10.4	100	0.26
Iodine chloride (β)	ICl (β)	13.9	56	n.a.
Molybdenum Fluoride	MoF ₆	17	50	n.a.
Sulfur trioxide (α)	SO ₃ (α)	17	108	n.a.
Iodine chloride (α)	ICl (α)	17.2	69	n.a.
Tetraphosphorus hexaoxide	P ₄ O ₆	23.7	64	n.a.
Phosphoric acid	H ₃ PO ₄	26	147	0.434[16]
Arsenic bromide	AsBr ₃	30	38	n.a.
Tin bromide	SnBr ₄	30	28	0.0859
Boron iodide	BI ₃	31.8	10	n.a.
Sulfur trioxide (β)	SO ₃ (β)	32.3	151	n.a.
Titanium Bromide	TiBr ₄	38.2	23	n.a.
Hypophosphoric acid	H ₄ P ₂ O ₆	55	213	n.a.
Sulfur trioxide (γ)	SO ₃ (γ)	62.1	331	n.a.
Antimony trichloride	SbCl ₃	73.4	25	n.a.
Sodium nitrate	NaNO ₃	307	199	0.51
Potassium nitrate	KNO ₃	380	266	0.45
Potassium hydroxide	KOH	380	149	n.a.

Table 5: Melting temperature and latent heat of metallic PCMs

Name	T_m (°C)	H (kJ/kg)	k (W/m·K)	ρ (kg/m ³)	Cp (kJ/kg)
Mercury	-38.87	11.4	8.34	13546	0.139
Cesium	28.65	16.4	17.4	1796	0.236
Gallium–gallium antimony	29.8	n.a.	n.a.	n.a.	n.a.
Gallium	30	80.3	29.4	5907	0.37
Rubidium	38.85	25.74	29.3	1470	0.363
Bismuth-lead-indium-tin-cadmium (Bi _{44.7} Pb _{22.6} In _{19.1} Sn _{8.3} Cd _{5.3})	47	36.8	15	9160	0.197
Bismuth-indium-lead-tin (Bi ₄₉ In ₂₁ Pb ₁₈ Sn ₁₂)	58	28.9	10	9010	0.201
Cerrow	58	90.9	n.a.	n.a.	n.a.
Bismuth-cadmium-indium	61	25	n.a.	n.a.	n.a.
Potassium	63.2	59.59	54.0	664	0.78
Cerrobend	70	32.6	n.a.	n.a.	n.a.
Bismuth-lead-tin-cadmium (Bi ₅₀ Pb _{26.7} Sn _{13.3} Cd ₁₀)	70	39.8	18	9580	0.184
Bismuth-lead-indium	70	29	n.a.	n.a.	n.a.
Bismuth-indium	72	25	n.a.	n.a.	n.a.
Bismuth-lead-tin (Bi ₅₂ Pb ₃₀ Sn ₁₈)	96	34.7	24	9600	0.167
Bismuth-lead-tin	96	n.a.	n.a.	n.a.	n.a.
Sodium	97.8	n.a.	n.a.	n.a.	n.a.
Bi–Pb	125	n.a.	n.a.	n.a.	n.a.
Bismuth-tin (Bi ₅₈ Sn ₄₂)	138	44.8	19	8560	0.201
Indium	156.8	28.59	36.4	7030	0.23
Lithium	186	433.78	41.3	515	4.389
Tin-zinc (Sn ₉₁ Zn ₉)	199	32.5	61	7270	0.272
Tin	232	60.5	15.08	730	0.221
Bismuth	271.4	53.3	8.1	979	0.122

Table 6: Thermophysical properties of eutectic PCMs

Name	Composition (wt. %)	T _m (°C)	H (kJ/kg)
Diethylene glycol	n.a.	-10	247
Tetradecane+octadecane	n.a.	-4.02	227.52
Water+polyacrylamide	n.a.	0	295
Tetradecane+docosane	n.a.	1.5-5.6	234.33
Tetradecane+hexadecane	91.67+8.33	1.7	156.2
Tetradecane+geneicosane	n.a.	3.54–5.56	200.28
Na ₂ SO ₄ +NaCl+KCl+H ₂ O	31+13+16+40	4	234
Tetrahidrofurano (THF)	n.a.	5	280
Pentadecane+heneicosane	n.a.	6.23-7.21	128.25
Pentadecane+docosane	n.a.	7.6-8.99	214.83
Pentadecane+octadecane	n.a.	8.5-9.0	271.93
Na ₂ SO ₄ +NaCl+NH ₄ Cl+H ₂ O	32+14+12+42	11	n.a.
C ₅ H ₅ C ₆ H ₅ +(C ₆ H ₅) ₂ O	26.5+73.5	12	97.9
Triethylolethane+water+urea	38.5+31.5+30	13.4	160
CaCl ₂ ·6H ₂ O+CaBr ₂ ·6H ₂ O	45+55	14.7	140
Na ₂ SO ₄ +NaCl+H ₂ O	37+17+46	18	n.a.
Capric + lauric acid	61.5+38.5	19.1	132
Capric + lauric acid	82+18	19.1-20.4	147
Capric + lauric acid	45+55	21	143
Capric+myrstic	73.5+26.5	21.4	152
Capric+palmitate	75.2+24.8	22.1	153
Na ₂ S ₄ +MgSO ₄ +H ₂ O	25+21+54	24	n.a.
C ₁₄ H ₂₈ O ₂ +C ₁₀ H ₂₀ O ₂	34+66	24	147.7
CaCl ₂ ·6H ₂ O +MgCl ₂ ·6H ₂ O	50+50	25	95
CaCl ₂ ·6H ₂ O+Nucleat+MgCl ₂ ·6H ₂ O	66.7+33.3	25	127
CaCl ₂ + NaCl + KCl + H ₂ O	48+4.3+0.4+47.3	26.8	188
Capric+stearate	86.6+13.4	26.8	160
CH ₃ CONH ₂ +NH ₂ CONH ₂	50+50	27	163
Triethylolethane+urea	62.5+37.5	29.8	218
Ca(NO ₃) ₂ ·4H ₂ O+Mg(NO ₃) ₂ ·6H ₂ O	47+53	30	136
CH ₃ COONa·3H ₂ O+NH ₂ CONH ₂	40+60	30	200.5
Lauric+palmitic acid	69+31	35.2	166.3
NH ₂ CONH ₂ +NH ₄ NO ₃	53+47	46	95
Mg(NO ₃) ₂ ·6H ₂ O+NH ₄ NO ₃	61.5+38.5	52	125.5
Mg(NO ₃) ₂ ·6H ₂ O+MgCl ₂ ·6H ₂ O	58.7+41.3	59	132.2
Mg(NO ₃) ₂ ·6H ₂ O+MgCl ₂ ·6H ₂ O	50+50	59.1	144
Mg(NO ₃) ₂ ·6H ₂ O+Al(NO ₃) ₃ ·9H ₂ O	53+47	61	148
CH ₃ CONH ₂ +C ₁₇ H ₃₅ COOH	50+50	65	218
Mg(NO ₃) ₂ ·6H ₂ O+MgBr ₂ ·6H ₂ O	59+41	66	168
Napthalene+benzoic acid	67.1+32.9	67	123.4
AlCl ₃ +NaCl+ZrCl ₂	79+17+4	68	234
AlCl ₃ +NaCl+KCl	66+20+14	70	209

$\text{NH}_2\text{CONH}_2+\text{NH}_4\text{Br}$	66.6+33.4	76	151
$\text{LiNO}_3+\text{NH}_4\text{NO}_3+\text{NaNO}_3$	25+65+10	80.5	113
$\text{LiNO}_3+\text{NH}_4\text{NO}_3+\text{KNO}_3$	26.4+58.7+14.9	81.5	116
$\text{LiNO}_3+\text{NH}_4\text{NO}_3+\text{NH}_4\text{Cl}$	27+68+5	81.6	108
$\text{AlCl}_3+\text{NaCl}+\text{KCl}$	60+26+14	93	213
$\text{AlCl}_3+\text{NaCl}$	66+34	93	201
$\text{NaNO}_2+\text{NaNO}_3+\text{KNO}_3$	40+7+53	142	n.a.

Table 7: MEPCM/NEPCM fabricated by in-situ polymerization

Core	Shell	References
Tetradecane	Melamine formaldehyde (MF)	Choi[24]
Tetradecane	Urea formaldehyde (UF)	Fang[25]
Tetradecane	1) PVAc (polyvinyl acetate) 2) PS (poliestirene) 3) Polymethyl methacrylate (PMMA) 4) Polyethyl methacrylate (PEMA)	Yang[26]
Paraffin	UF	Jin[27]
n-octadecane	UMF/UF/MF	Zhang[65]
n-octadecane	MF	Li[29], Zhang[23], Zhang[28]
Fragrant Margin oil	MF	Hong[30]
n-hexadecane and n-eicosane	MF	Salaün[31]
n-octadecane	Polystyrene	Fang [66]
Bromo-hexadecane	Aminoplast	Song[32]
n-Octadecane	Polyurea (TDI-EDA/DETA/Jeffamine T403)	Zhang[34], Cho[37], Siddhan[38], Su[39]
Butyl stearate	Polyurea (TDI-EDA)	Chen[35]
Hexadecane	Polyurea (TDI-EDA)	Zou[36]
n-pentadecane/n-eicosane/ paraffin	UF	Tseng[40]
n-Hexadecane	Polystyrene	Y.F. Ai [44]
Paraffin wax PRS, tetradecane, Rubitherm 20, nonadecane	Polystyrene	Sánchez[45] [46]
n-Octadecane	Polystyrene	You[47] [48], Li[49]
n-Octadecane	Polydivinylbenzene (PDVB)	Chaiyasat[50]
n-Ocatdecane	MMA-BDDA, MMA-DVB, MMA-TMPTA, MMA-PETRA	Qiu[51]
Paraffin, methyl stearate	Polyurethane	Cheng[52]
n-Docasane	PMMA	Alkan[54], Chen[61]
n-Eicosane	PMMA	Alkan[55]
n-Octadecane	PMMA	Sari[57]
n-Heptadecane	PMMA	Sari[56]
Paraffin	PMMA	Ma[58]
n-Hexadecane	PMMA	Alay[59]
Paraffin	Polystyrene	Luo[60]
n-Hexadecane	UF	Li[62]
Paraffin wax RT 80	styrene-butyl acrylate (St-BA)	Fuensanta[63]

Palmitic acid (PA)
Paraffin

Aluminium hydroxide
Silicon dioxide

Pan[42]
Li[43]

Table 8: Statistics results of MEPCM/NEPCM via various encapsulation technologies

Microencapsulation method	Diameter [μm]	Core content (%)	Encapsulation efficiency (%)
In-situ interfacial polymerization	0.5–1000	29-80	71-87
In-situ suspension polymerization	0.72-237	20-75.3	78-100
In-situ emulsion polymerization	0.14-2	28-61	82.6
In-situ miniemulsion polymerization	0.1–0.5	8-60	80-82.2
Complex coacervation	2–1200	26-67	80-95
Sol-gel encapsulation	2–30	46-74	82-90.7
Phase separation method	0.5–1000	43-75	66–75
Solvent extraction/evaporation methods	0.5-10	43-53	56-64